ASSOCIAÇÃO EURATOM/IST

IST/Instituto de Sistemas e Robótica

Geometric Feasibility of the ITER Air Cushion Remote Handling Casks and Extensions for Free Roaming Navigation

Final Report

Maria Isabel Ribeiro, Pedro Almeida Lima, Pedro Miguel Aparício
{*mir,pal,aparicio*}*@isr.ist.utl.pt*

June, 1998

List of Figures

Notation

- **Cask** - container that will accommodate the materials to be transported.
- **Platform** - motorized vehicle, separated from the cask, that will carry the cask.
- **AGV** - Automatic Guided Vehicle.
- **PLC** - Programmable Logic Controller.
- **HCB** - Hot Cell Building.
- **TB** - Tokamak Building.
- **VV** - Vacuum Vessel.
- **RHC** - Remote Handling Casks.
- **HCI** - Human Computer Interface.
- **LGV** - Laser Guided Vehicle.

1 Introduction

As a result of previous work [IST97], the concept of an air cushion vehicle using an inductive AGV solution for primary guidance and navigation has been selected as the ITER reference for transport of components between the TB and the HCB. This choice has been made considering the flexibility of the solution (easy modification of the transport path), the current state-of-the-art and the expected lower cost with respect to the alternatives considered — in particular a rail-based solution.

This report presents some of the issues involved in the design of the cask transporter system for ITER, namely the path topology, the areas spanned by the platform during motion and the clearance for removing it from underneath the cask, this leading to a discussion on the constraints that have to be satisfied in the building design.

An open discussion and further studies are being carried out to extend, in the long term, the AGV fixed guidance proposed in [NNC98] [AeroGo98] to a free roaming vehicle, able to leave the physical path and to regain it again, should this be necessary during operation. This report discusses the general conditions regarding navigation, guidance and path planning under which an AGV type platform can operate as a free-roaming vehicle or as a mixed-type vehicle.

1.1 Objectives

NNC has pointed towards a solution for the ITER RH transport vehicles with a platform separated from the cask [NNC98]. Rescue and cost are the most important reasons pointed out to favor the separated solution: should the platform be able to move by itself without carrying the cask, rescue operations will be easier and total cost will be reduced because the number of platforms can be less than the number of casks. In a previous report [IST97], IST concluded that a rhombic kinematic configuration with two drive-and-steering wheel blocks (denoted as *drive units* in [AeroGo98]) would be the most appropriate solution for such a platform.

In this report, geometric considerations relative to the rhombic platform are presented, with the objective of determining whether impact to the building or to vehicle design exists or not. Two main topics are discussed:

- the area spanned by the platform when following a specially designed path for particular/critical areas on the buildings;
- the clearance required to remove from and insert the platform underneath the cask;

The study leads to conclusions on the geometric feasibility of the rhombic kinematic structure, given the actual building design and the path to be followed. Critical points along the path are pointed out allong with suggested solutions.

Another objective of this document is to provide some general considerations regarding the navigation and guidance systems that will integrate the vehicle, should it operate in a free-roaming mode.

1.2 Organization

In Section 2, the geometric feasibility of the rhombic kinematic platform is analysed for the six main regions which compose the path between the VV and the HCB, considering two main issues: recommended path and spanned area, and rescue clearance. The operating principle of a vehicle with a primary and a secondary navigation systems, which can switch between a free-roaming and an AGV mode of operation, is discussed in Section 3 as an extension of the solution proposed in [AeroGo98]. Three appendices describe the geometry of the rhombic kinematic structure, the derivations to compute the rescue clearance associated to the vehicle in the TB gallery and the HC transport corridor, and those to compute the vehicle spanned area in the TB gallery, respectively. A short appendix gives some insight on cubic spirals-based path planning. The equations in those appendices are widely used in Section 2, so the interested reader may wish to consult them first. A final appendix contains the specification sheet of a laser-scanner navigation system.

2 Geometric Feasibility Study

Along the route between the TB and the HCB, the air cushion vehicles must follow different path types within the available space, perform some manoeuvres, and overcome some critical locations, for which the feasibility of rescue manoeuvres has to be carefully analysed.

Safety and rescue are key issues in ITER. Equipment failures are supposed to occur rarely (i.e., the RH transportation system must be very reliable), but it should always be possible to recover from any kind of failure preventing the vehicle from pursuing its motion along the planned path. To improve system safety, the concept of an air cushion motorized platform carrying a transport cask was developed. Under this concept, should a problem arise (e.g., failure of air supply), it is possible in most cases to remove the platform from underneath the cask, as the latter is self-supported by fixed lateral feet, raised when the air casters are operational. When the geometry of the vehicle and walls relative positions prevents platform removal, different rescue procedures will be required, depending on the type of problem. Typically, should the stopping condition be caused by an event other than an aerocaster or air supply failure, the backup manual mode (see below) can be used to move the vehicle to a pose (position + location) where the platform can be removed and replaced by a new one. Otherwise a rescue vehicle will be needed to provide air supply, so that the above manoeuvre can be carried out.

In this report, we are mainly concerned with the geometric feasibility of the air cushion RHC described in [AeroGo98]. This includes planning smooth paths to increase safety and to simplify guidance control, the verification of possible overlaps between the vehicle spanned area and the building walls when following a planned path, and the analysis of the clearance required to remove the platform from underneath the cask in different possible failure locations. Recommendations regarding impact on the building and on vehicle design are the most important result of this study.

2.1 Main assumptions

It is assumed that the platform is rigid and can only move on a straight line along its longitudinal axis when coming out from or entering underneath a cask. No other type of platform manoeuvres are considered while part of its body is still underneath the cask. Nevertheless, a multi-body segmentation (e.g., 2 or 3 segments) of the platform is envisaged as an improved solution to recover from air compressor failures by removing the shorter modules one at a time. As such, different clearances, depending on module length, will be considered in the rescue manoeuvres subsections. Notice that the platform may follow almost any path topology when it is completely underneath the cask or when there is no cask on it. Also, studies regarding the rescue clearance assume always that the platform may only leave from underneath the cask moving backwards (i.e., the rear, shown in Figure 1 is the leading platform side during motion).

To evaluate spanned areas and rescue clearances, the vehicle dimensions, shown in

Figure 1, are those presented in [AeroGo98], i.e.,

- platform length (including the platform rear space for the control system, shown on the left of the figure) $l = 8500$ mm,
- platform width $w = 4000$ mm,
- distance between drive units $l' = 6300$ mm[1]

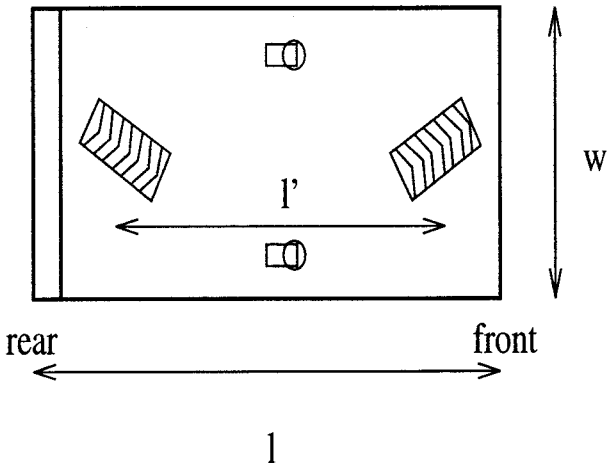

Figure 1: Schematic representation of a rhombic vehicle.

Alternative values for l' (e.g., 5000 mm) were tested to search for possible improvements on the total spanned areas.

All building dimensions were obtained or extrapolated from the most recently available ITER-EDA drawings (end of 1997). In what concerns free space for vehicle motion, the maximum and minimum considered radii of the TB gallery boundary circles are $r_{max} = 42$ m and $r_{min} = 32$ m, respectively. The width of a typical VV docking port entrance is 5000 mm. The laydown hall entrance closer to the lift is 4900 mm wide. Laydown hall width is 10250 mm. Its length is 20100 mm. The HC transport corridor is 4700 mm wide in the initial 46000 mm, and 6000 mm wide in the remaining 93725 mm. Inside the HCB, only the last docking port is considered, since it corresponds to the most difficult situation, from a geometric standpoint. Its entrance is 5500 mm wide.

In [NNC98], 3 operation modes are considered for the air cushion RHC:

1. **semi-automatic**, used when the AGV follows a track under normal operation, controlled by the on-board PLC;

[1] The 6300 mm value for l' was based on earlier drafts of [AeroGo98]. However, should the current design with two possible values for l' (6075 and 6700 mm), be accepted, the simulation tool can be used to update the results presented in this report.

2. **backup manual**, used as a backup when the on-board PLC fails, with a reduced set of operator functions (e.g., speed control) available to the operator;

3. **normal manual**, used for operator controlled manoeuvres, with an available "high-level" set of operator actions (e.g., individual or both wheels steering, crab steering, turning on the spot).

In mode 1, a maximum deviation from the track of ± 3 mm is anticipated, while a maximum deviation from the track of ± 100 mm might occur in mode 3, when the operator is driving the vehicle to follow the track. Mode 3 is used for rescue vehicles and remote manoeuvres carried out by the operator.

This section tackles the spanned area and rescue clearance issues for the six main regions composing the path between the TB and the HCB: the VV docking ports, the TB gallery, the path from the lift to the laydown hall, the path from the laydown hall to the HC transport corridor, the HC transport corridor, and the HCB docking ports. The analysis of each region corresponds to a subsection. For each of them, results from simulations done in Matlab are presented showing the recommended path with the corresponding spanned area and the rescue space for vehicle manoeuvres, should an equipment failure occur. Some results are based on closed form expressions derived in Appendices B and C, others are computed on the fly, at simulation time. In both cases, simulations are parameterized by the vehicle and building dimensions, hence it is possible to cope with possible modifications. The studies made concentrated on determining smooth paths to be followed by both steering wheels, so that "ad-hoc" and/or operator-driven manoeuvres could be avoided. Manoeuvres are a possible alternative in most cases (and are compared with smooth paths for a few regions), as well as separate paths for the two steering wheels. Nevertheless, we consider the smooth single path as the most desirable solution, since it is based on an analytical smoothness criterion which can be applied to practically all cases.

Results concerning rescue will consider the worst case anticipated scenarios for vehicle misalignment after the occurrence of a failure, i.e.,

- for the deviation error d: both wheels deviated $+100$ mm from the track:
- for the orientation error β: one of the wheels deviated $+100$ mm from the track, the other wheel deviated -100 mm from the track.

Please check Appendices B and C for a clear definition of d and β.

2.2 VV docking ports

2.2.1 Recommended path and spanned area

The path between the TB gallery and the VV docking ports is characterized, in the typical cases, by switching from a 37 m radius circular path to a radial path (or backwards). The

vehicle manoeuvre is even harder due to the narrow entrance to the docking ports and the relatively narrow space in the TB gallery. However, simulations show (see Figure 2) that it is possible to find a cubic spiral path, as explained in Appendix D, to overcome the switching smoothly and without colliding with the gallery and docking ports walls, even in the worst case of a ± 100 mm vehicle deviation from the path.

The results shown in this subsection were selected from a set of simulations where different paths and two distances between drive units ($l' = 5000,\ 6300$ mm) were considered.

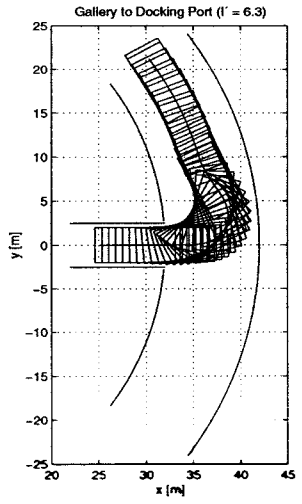

Figure 2: **Vehicle recommended path and spanned area when** moving from the gallery to a VV docking port (**scenario 1**).

2.2.2 Rescue Clearance

The space available for **rescue manoeuvres was** studied for two different scenarios:

1. the vehicle follows **the path suggested** in the previous subsection;
2. the vehicle follows the **gallery circular** path, stops at the entrance of a docking port access corridor, and rotates **90° about** its center (*turns on the spot*), to align itself with the access corridor (see **Figure** 5). This is similar to the use of turn-tables for rail systems.

Results concerning scenario 1 are illustrated in Figure 3. The plot shows the evolution of the worst case clearance ($\overline{AA'}$ in Appendix B, see Figure 32) along the path shown in Figure 2. In the figure, motion in both directions is made in such a way that the platform front faces the VV docking port door when the vehicle is docked. The iteration number in the x-axis label refers to the simulation steps depicted in Figure 3 as successive vehicle

locations. From the plot, it can be seen that there are locations along the path (roughly iterations 14 to 32) where, should the vehicle stop due to some malfunction, it would not be possible to remove the platform from underneath the cask, because the clearance is below 8.5 m, the total length of the platform plus the platform rear space for the control systems. With a 2-body platform, and considering a 4.5 m long body to include the additional rear space for the control system, the range of locations for which this type of rescue would not be possible is reduced (roughly iterations 15 to 27), as theoretically each body could be removed at a time. Notice that platform removal is possible for all the other locations. Vehicle position and orientation at the critical locations, between which platform removal is not possible (i.e., 14 and 32 for a 1-body platform, 15 and 27 for a 2-body platform), are depicted in Figure 4.

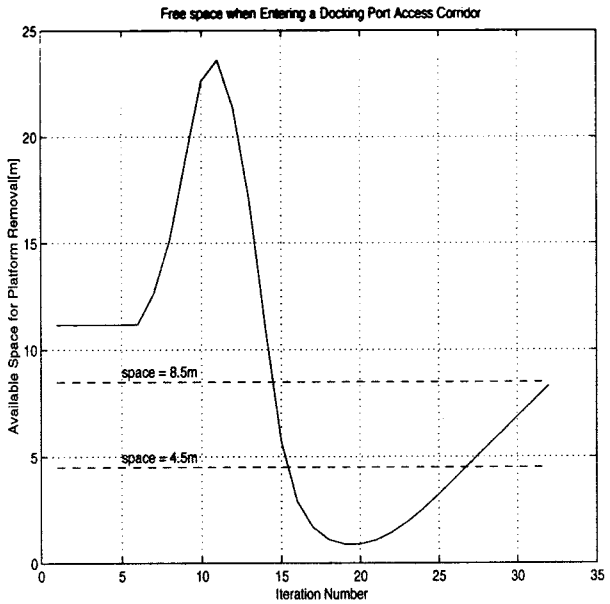

Figure 3: Clearance space available while moving from the gallery to a VV docking port, following a smooth path (scenario 1). The minimum corresponds to *space* = 880 mm.

.

The study regarding scenario 2 was based on the expressions (20) and (23), derived in Appendix B. The clearance *space* was studied for several values of the orientation error β, in the cases where no radial deviation from the path ($d = 0$) was considered. In this case, β is not exactly an error with respect to the track, but results exclusively from vehicle manoeuvring. Nevertheless, the angles are measured according to Figure 32 of Appendix B. A general rotation on the spot from 0 to +90° has been considered for the manoeuvres, and the clearance *space* values were determined from the expressions in Appendix B.

Turning on the spot with the vehicle centered on the 37 m radius circular trajectory allows a clearance whose minimum value is 80 mm. Therefore, this is a problematic

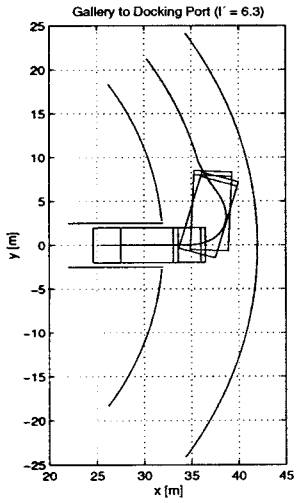

Figure 4: Vehicle pose at critical iterations 14, 15, 27 and 32 (scenario 1).

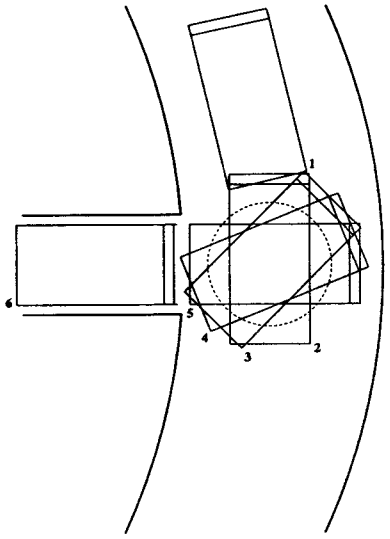

Figure 5: Vehicle manoeuvres to move from the gallery to a VV docking port.

manoeuvre, as a malfunction during rotation would prevent rescue by immediate platform replacement. Actually, in general, clearance is enough for a 1-body vehicle when $-23° < \beta < 4°$ and for a 2-body vehicle when $-26° < \beta < 11°$.

Comparing the two possible scenarios, we recommend scenario 1 since, despite of similar rescue problems, it is the one requiring less operator-driven manoeuvres and is based on a smoother path.

2.3 In the TB gallery

2.3.1 Recommended path and spanned area

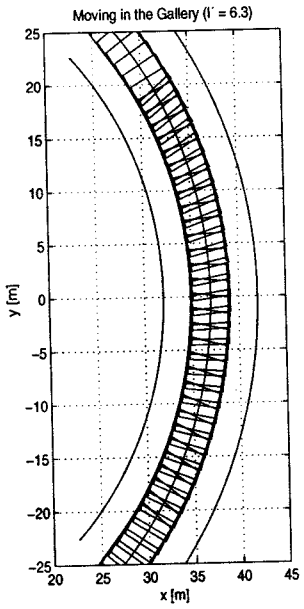

Figure 6: Vehicle path and spanned area when moving in the TB gallery.

The recommended path in the TB gallery is a circular arc concentric with the gallery inner and outer boundaries, and equidistant to them, i.e., with a radius of $r_{traj} = 37$ m. Part of the path and vehicle spanned area are shown in Figure 6.

A study was made regarding the distance to the outer and inner gallery walls of their closest vehicle points, respectively $r_{max} - \overline{OA}$ and $\overline{OC} - r_{min}$ (see Appendix C, Figure 35). The following table presents the results obtained for combinations of the worst case deviation and orientation errors with respect to the track. No space problems are noticeable.

d [m]	β [°]	Distance to the walls [m]	
		Outer Wall	Inner Wall
0.1	-2	2.89	2.99
	0	2.74	3.00
	2	2.59	3.99
0.0	-2	2.99	2.89
	0	2.84	2.90
	2	2.69	2.89
-0.1	-2	2.79	3.09
	0	2.64	3.10
	2	2.49	3.09

2.3.2 Rescue Clearance

The following table was built from Equation (14), derived in Appendix B, thus assuming the vehicle aligned with the track. It shows the clearance space available for platform removal/insertion, under two possible values for r_{max}. We made an exercise of reducing the radius of the outer wall, to take into account some uncertainty on gallery column dimensions.

r_{max} [m]	42	41
clearance *space* [m]	11.08	9.59

Note that the available space for the $r_{max} = 42m$ is the same that is shown in the left-most side of Figure 3, i.e., the plot segment corresponding to the vehicle motion in the gallery. When the radius was reduced to $41m$, the space became considerably smaller, as shown in the table. Nevertheless, for both values of r_{max}, the clearance is enough for both platform removal/insertion and/or rescue vehicle manoeuvring in the vehicle vicinity.

When the vehicle is not aligned with the track, results for the zero and worst case deviation d and orientation β are shown in the following table, and were computed from Equation (20) in Appendix B.

d [m]	β (°)	Clearance *space* ($\overline{AA'}$)[m]
-0.1	-2	12.69
	0	11.33
	2	10.10
0.0	-2	12.43
	0	11.08
	2	9.83
0.1	-2	12.18
	0	10.83
	2	9.59

Again, for all situations, there is enough space for platform removal/insertion.

2.4 From the lift to the laydown hall

2.4.1 Recommended path and spanned area

This section presents a cubic spiral path (see Appendix D) to be followed when the vehicle moves between the TB gallery lift and the laydown hall. The simulation results are plotted in Figure 7. From the figure one can conclude that there is scarcely space to move along the path without bumping into the laydown hall entrance walls. Nevertheless, the current drawings are unclear regarding lift dimensions and location. The path depends strongly on this, since the vehicle must leave completely the lift before turning to the laydown hall entrance, so as to avoid colliding with the lift columns/walls. As such, building modifications are required to increase the free space for vehicle motion.

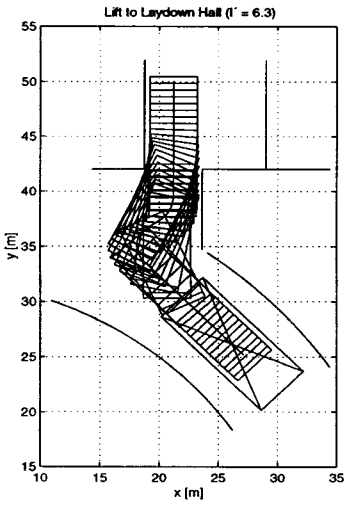

Figure 7: Vehicle spanned area when moving from the lift to the Laydown Hall

2.4.2 Rescue Clearance

There is enough space between the lift and the laydown hall to assume the existence of rescue clearance in most cases. However, the dimensions and locations of some columns inside and outside the lift remain unclear and could cause problems. Critical points might be the columns at the lift exit, whose dimensions are unclear, and the entrance of the laydown hall. In any case, manoeuvres would always be an alternative to the proposed smooth path.

2.5 From the laydown hall to the HC transport corridor

2.5.1 Recommended path and spanned area

A manoeuvre-based strategy to move the vehicle between the laydown hall and the HC corridor is depicted in Figure 8. Under this strategy, the vehicle follows a straight line inside the laydown hall until it reaches location 2. There, both wheels are rotated 90°, so as to let the vehicle move sideways until location 3, where its central point is located equidistant from the laydown hall walls. At this location, the vehicle turns on the spot 90° clockwise, through locations 4–6. From location 6, a new sideways motion is performed until location 7 is reached. At this location, the vehicle is ready to follow the HC transport corridor straight line path.

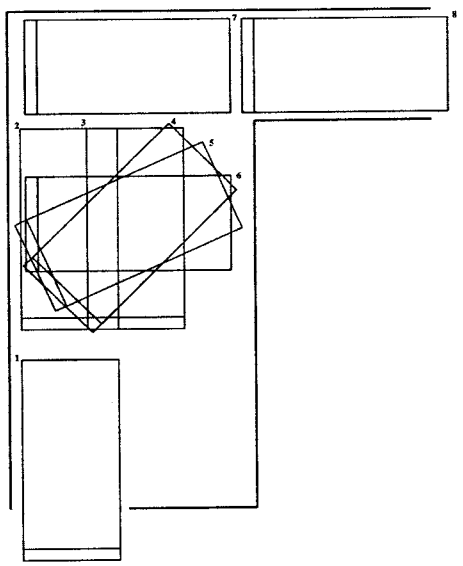

Figure 8: Vehicle manoeuvres to move from the laydown hall to the HC transport corridor.

This strategy, besides involving several manoeuvres which require operator intervention, may cause serious rescue problems in case of an air cushion failure, since the platform (or the platform segments) would not have enough clearance to be removed from underneath the cask, in most situations.

Figure 9 illustrates the use of cubic spirals to implement such a manoeuvre. In Figure 9-a), only one path for both wheels was used. Under this scenario, collision is unavoidable, for the current building configuration. When separate paths for each wheel are used (see Figure 9-b)) there is no collision, but the available space is reduced. Furthermore, there is no criterion to quantify the smoothness of the vehicle motion in this case. Various paths were generated and tested, but none was able to cope with the walls strong geometrical constraints.

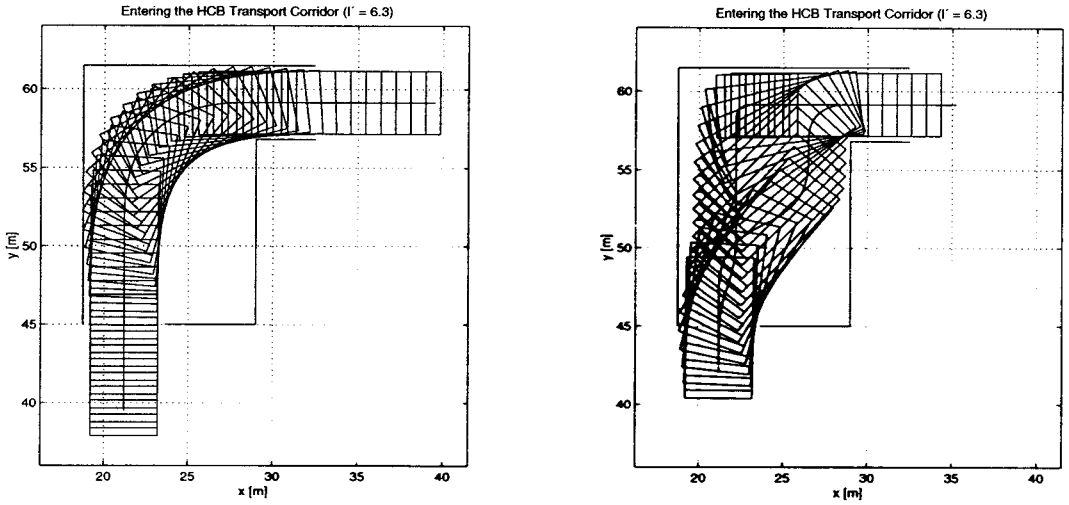

a) b)

Figure 9: Vehicle spanned area while moving from the laydown hall to the HC transport corridor: a) with one path for both wheels; b) with separated paths.

2.5.2 Rescue Clearance

Figure 10 presents the available space to perform rescue manoeuvres when the vehicle enters the HC corridor. Those values are related to the manoeuvre presented in Figure 9-a). It can be seen that, as the vehicle moves parallel to the left wall, the space is very large (above 25 meters). As soon as it starts to turn in order to enter the HC corridor, the available space is quickly and progressively reduced until collision occurs. When the vehicle enters the HC corridor and gets aligned with it, the rescue available space increases again, as the vehicle moves into the corridor. Minor modifications to the building are required, both regarding the laydown hall and the HC corridor widths, so as to cope with this clearance requirement.

In Figure 10, one can identify a range of vehicle locations along the path for which neither a 1-body nor a 2-body platform would be removable from underneath the cask. Again, the range is smaller for the 2-body solution. Figure 11 shows the vehicle pose at the critical locations 11 and 29 (for a 1-body platform), and 12 and 24 (for a 2-body vehicle).

The best path obtained using cubic spirals, shown in Figure 9-a), is the one which requires less building modifications and whose corresponding rescue clearance is larger.

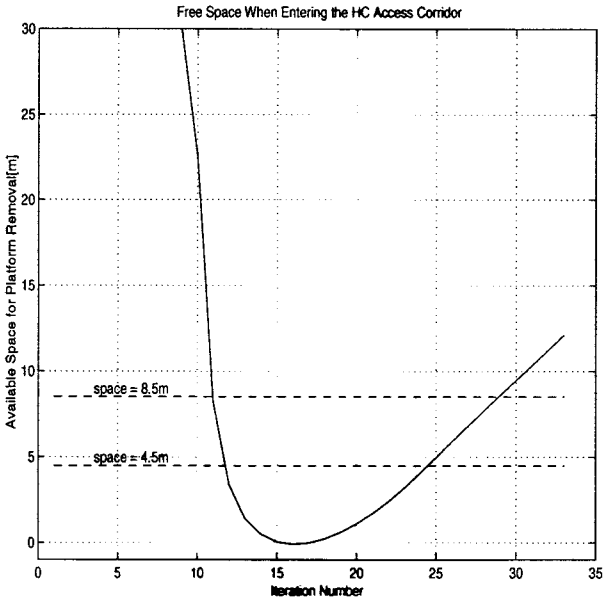

Figure 10: Clearance space available while moving from the Laydown Hall into the HC corridor. The minimum corresponds to $space = -90$ mm.

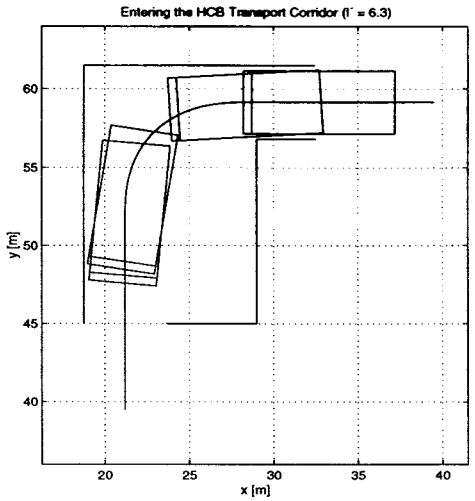

Figure 11: Vehicle pose at critical iterations 11, 12, 24 e 29.

2.6 HC transport corridor

2.6.1 Recommended path and spanned area

To move the vehicle in the transfer corridor, the recommended path is the straight line depicted in Figure 12. This path keeps the transporter in the middle of the available space. The free space on each side of the vehicle is 350 mm, when rotational or translational errors are not considered.

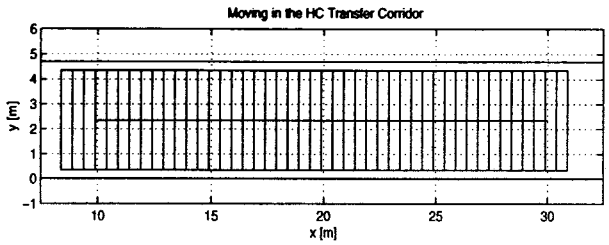

Figure 12: Vehicle spanned area when moving in the HC transfer corridor

2.6.2 Rescue Clearance

The following table presents the clearance available for rescue manoeuvres when the vehicle is moving in the Hot Cell Transfer Corridor, subject to a misalignment error. Detailed expressions for clearance can be found in Appendix B.

Clearance space [m]	$\beta = -1.5°$	$\beta = -1.0°$	$\beta = -0.5°$	$\beta = 0.5°$	$\beta = 1.0°$	$\beta = 1.5°$
d = 0.1 m	1.26	4.11	12.69	58.53	27.03	**16.53**
d = 0.0 m	8.89	15.57	35.61	35.61	15.57	**8.89**
d = -0.1 m	16.53	27.03	58.53	12.69	4.11	**1.26**

From those results, it is possible to conclude that, e.g., for $d = 0m$, should the vehicle orientation error be superior to 1.5°, the available space does not allow platform removal or insertion underneath the cask, for a 1-body platform. Notice that, for larger values of the error d, this will happen even for smaller values of β. Nevertheless, it should be pointed out that the worst case for the orientation error β is 2° (see Appendix B). This

means that a slightly wider corridor would allow immediate platform replacement even for the worst case misalignments.

2.7 Docking ports of the HCB

2.7.1 Recommended path and spanned area

This section presents the simulation results when the vehicle moves between the HC corridor and the HC docking ports. The last docking port was chosen for the simulations, because this is one of the narrowest entrances and it has an additional wall at the end of the first corridor.

Figure 13 illustrates this case. In the same figure, the proposed cubic spiral path is depicted. It is clear that with the current wall configuration, lateral and rear collision are unavoidable. Several additional paths were tested, but none was able to cope with the walls geometrical constraints. As such, building modification is required.

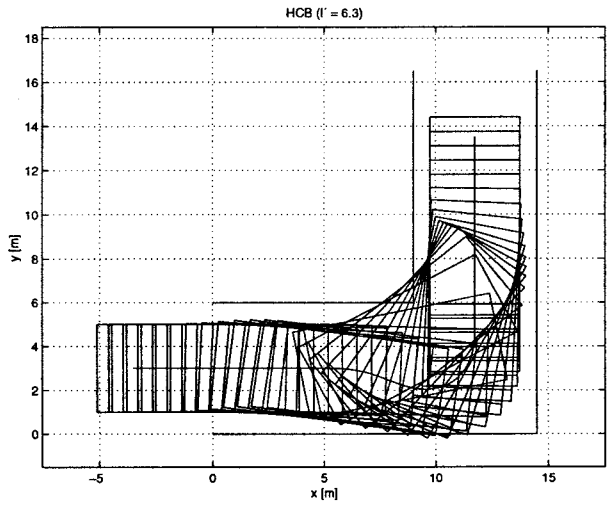

Figure 13: Vehicle spanned area in the HCB.

2.7.2 Rescue Clearance

Figure 14 presents the evaluation of the free space behind the transport cask, as it enters the docking port. It can be seen that the available space varies from more than 20000 mm to a collision scenario between the vehicle and the wall. To allow immediate platform replacement, building modification is required. Actually, even for a 2-body platform, rescue without switching to manual mode or requiring a rescue vehicle will not be possible between iterations 15 and 30, shown in Figure 15.

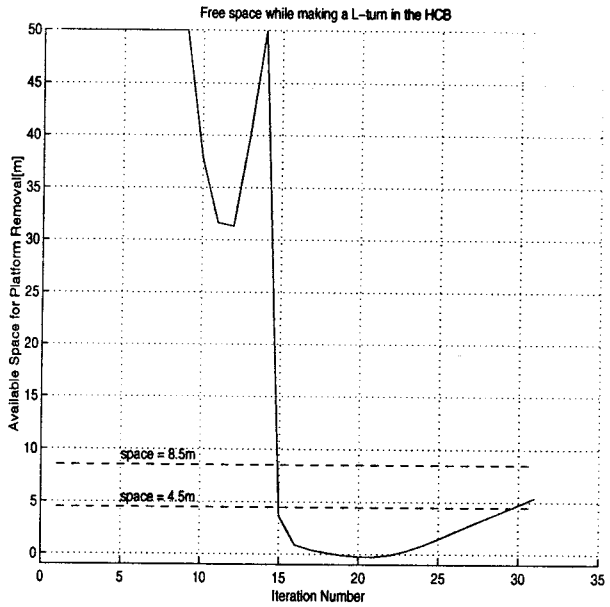

Figure 14: Clearance space available while moving into the HCB docking cell. The minimum corresponds to $space = -230$ mm.

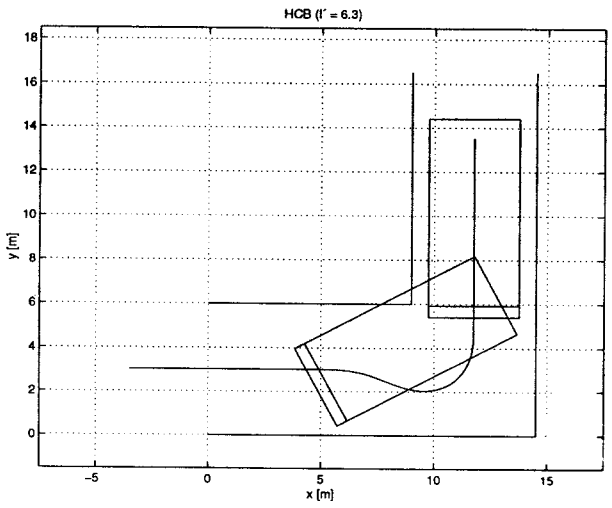

Figure 15: Vehicle pose at critical iterations 15 and 30. **showing limit cases of rescue** clearance availability for a 2-body platform.

2.8 Conclusions

The geometric feasibility study presented in this section leads to the following conclusions:

- The vehicle design proposed in [NNC98] is satisfactory from the standpoint of geometric feasibility. Even though geometric constraints are not satisfied for some critical locations along the path between the HCB and the VV, this is exclusively due to inappropriate building dimensions and could not be solved by modifications to the vehicle geometry and/or kinematic structure, assuming a rigid structure;
- Building modifications are required at some locations along the path, as mentioned in the text;
- Rescue vehicles will be needed for a small number of situations where building modification is not possible and, due to an aerocaster failure in a critical pose, neither clearance space is available for rescue by platform replacement nor the vehicle (cask + platform) is able to move backup manual mode;
- Smooth paths which either do not require or require only minor building modifications were determined for all 6 studied regions along the path, based on a cubic spirals method. Those paths do not require separate tracks to be followed by the vehicle drive units.

Some open points remain:

- Manoeuvres may be a valid (or the only possible) alternative to cubic spiral paths in some situations. Should they be considered preferable, a more thorough study of spanned areas and rescue clearance should be made.
- Another alternative are separate paths for the two steering wheels. It may even be possible to find a smoothness criterion to design them systematically, but such a study should only be done if single paths cannot solve the problem.

3 Navigation and Guidance of a Free-roaming platform

3.1 Introduction

The basic operational principle of any automated transporter, acting as an AGV or as a free-roaming vehicle is represented in Figure 16 where the shaded blocks have the following role,

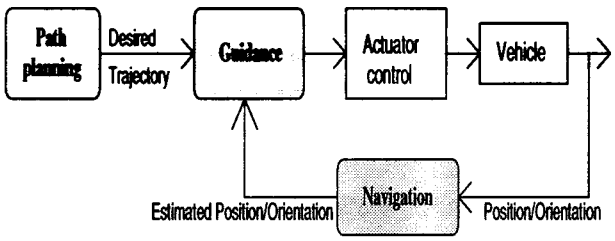

Figure 16: Integration of Navigation and Guidance

Path planning refers to either establishing a physical path, defined at floor level, or designing a virtual path. In both cases the path will act as a reference path to be followed;

Navigation refers to the estimation of the vehicle's location (position and orientation) relative to the physical path or to a world frame;

Guidance is the action of providing the set points to the vehicle controllers associated with the drive and steering wheels actuators. The action is taken based on the evaluation of the deviations (errors) from the reference path.

These operations are shared by any transporter irrespectively of the vehicle's kinematics. In the framework of the feasibility studies for an Air Flotation Transport System carried out in [IST97], [AeroGo98], a rhombic configuration was proposed and will be assumed in the sequel. Any change on this option or on the transporter dimensions will not modify the results and discussions presented in this section.

Various degrees of freedom may be achieved with different combinations of path reference design and navigation methodologies. A set of possible combinations is displayed in Table 1

Regarding the guidance and navigation solutions, an AGV type vehicle is proposed in [AeroGo98], which means that, besides the manoeuvres remotely controlled by an human operator, the transporter follows a physical path defined by a 50mm wide steel guiding

stripe installed at floor level. In this case, the reference path for semi-automatic operation mode is defined beforehand, and the **Path Planning** block displayed in Figure 16 plays no role during on-line operations. The path topology, i.e., the set of all possible reference routes, has to be defined a priori taking into account the desired final destinations, the vehicle dimensions and kinematics and the building design. Key issues for this definition are the requirements of smooth trajectories and the areas spanned by the transporter along the routes.

In this AGV type of vehicle, the **Navigation** block in Figure 16 evaluates the vehicle location information relative to the metal stripe, this being achieved by a set of two independent antennas. The transporter orientation relative to the metal stripe is straightforward computed from the distance between the two antennas and the deviation sensed by each of them. Additional qualitative location relative to the stripe is provided by the video signal chosen from a set of four video cameras installed in the front and in the rear of the platform and pointing downwards. This signal is displayed in the operator control room. The absolute location along the stripe is obtained, at discrete points, by a set of transponders or bar codes installed at floor level at pre-specified locations. A detailed analysis should be carried out to define these locations. For this absolute location, qualitative information is additionally provided by the properly chosen video signal from the cameras installed on the environment along the platform's routes.

<table>
<tr><th></th><th>AGV
(semi-automatic mode)</th><th>LGV</th><th>Free-Roaming</th></tr>
<tr><td rowspan="3">Path-Planning</td><td rowspan="3">PHYSICAL PATH

metal stripe defining
the path topology</td><td colspan="2">VIRTUAL PATH</td></tr>
<tr><td>CAD designed
a priori</td><td>Computer Optimization
on-line</td></tr>
<tr><td colspan="2">downloaded to controller</td></tr>
<tr><td rowspan="2">Navigation</td><td>PRIMARY NAVIGATION</td><td colspan="2">SECONDARY NAVIGATION</td></tr>
<tr><td>W-sensor

Localization
relative to the
physical path</td><td colspan="2">Laser Scanner

Localization
relative to a
global frame</td></tr>
</table>

Table 1: Degrees of flexibility

stripe installed at floor level. In this case, the reference path for semi-automatic operation mode is defined beforehand, and the **Path Planning** block displayed in Figure 16 plays no role during on-line operations. The path topology, i.e., the set of all possible reference routes, has to be defined a priori taking into account the desired final destinations, the vehicle dimensions and kinematics and the building design. Key issues for this definition are the requirements of smooth trajectories and the areas spanned by the transporter along the routes.

In this AGV type of vehicle, the **Navigation** block in Figure 16 evaluates the vehicle location information relative to the metal stripe, this being achieved by a set of two independent antennas. The transporter orientation relative to the metal stripe is straightforward computed from the distance between the two antennas and the deviation sensed by each of them. Additional qualitative location relative to the stripe is provided by the video signal chosen from a set of four video cameras installed in the front and in the rear of the platform and pointing downwards. This signal is displayed in the operator control room. The absolute location along the stripe is obtained, at discrete points, by a set of transponders or bar codes installed at floor level at pre-specified locations. A detailed analysis should be carried out to define these locations. For this absolute location, qualitative information is additionally provided by the properly chosen video signal from the cameras installed on the environment along the platform's routes.

<table>
<tr><th></th><th>AGV
(semi-automatic mode)</th><th>LGV</th><th>Free-Roaming</th></tr>
<tr><td rowspan="3">Path-Planning</td><td rowspan="3">PHYSICAL PATH

metal stripe defining
the path topology</td><td colspan="2">VIRTUAL PATH</td></tr>
<tr><td>CAD designed
a priori</td><td>Computer Optimization
on-line</td></tr>
<tr><td colspan="2">downloaded to controller</td></tr>
<tr><td rowspan="2">Navigation</td><td>PRIMARY NAVIGATION</td><td colspan="2">SECONDARY NAVIGATION</td></tr>
<tr><td>W-sensor

Localization
relative to the
physical path</td><td colspan="2">Laser Scanner

Localization
relative to a
global frame</td></tr>
</table>

Table 1: Degrees of flexibility

provide primary information when the vehicle deviates significantly from the metal stripe path or in case automatic rescue manoeuvres are required. Nevertheless, both navigation systems should be working simultaneously, and the navigator must be pooling them constantly in order to perceive the best position estimate and to prevent malfunctions. Also, aiming at increasing the information provided to the operator or to assist the primary navigation, the secondary navigation should always be present even in the AGV type of operation.

3.2 Primary Navigation

Commonly used guidepath techniques for AGVs may be classified under passive and active tracking. Active tracking includes the use of a guidewire buried on the floor, and it is the most commonly used technique in industry, [Hammond86]. A low-voltage, low-current, low-frequency AC signal is conducted through the wire. A small electromagnetic field is radiated from the wire and two inductive-type sensors on the vehicle are used as the guidance detectors. The signal magnitudes of the two sensors are compared, and as long as they are equal, the transporter is centered on the guidepath. If the vehicle begins to deviate, the sensed signal magnitudes are no longer equal, and the signal differences is then used to steer the vehicle back to the path, [Hammond86].

From the passive tracking strategies, the one supported on a metal stripe has been used quite often and was the one proposed in [AeroGo98]. The differential steering operational principle underlying the use of a steel guiding stripe installed at floor level is the same as the one described for inductive steering.

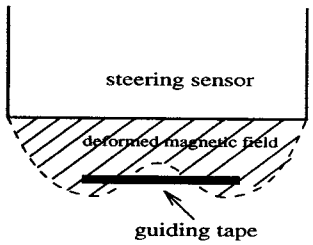

Figure 17: W-steering sensor

As represented in Figure 17, [Nuyts], a specially developed guiding sensor creates a W-form magnetic field. As described in the W-sensor specification sheet, [Nuyts], the presence of a $50mm$ wide steel guiding stripe affects the magnetic field characteristics, which can be measured and transformed into a correction signal to the steering motor. The represented W-sensor provides two output signals. With no metal being present, both outputs provide the same voltage. The presence of the guiding tape will cause both outputs to drop to a value which is proportional to the distance between the guiding tape and the sensor head. The lateral motion of the sensor head above the guiding tape will cause one output signal to rise, while the other output signal will lower at the same time.

If v_1 and v_2 are the output voltages of the two signals.

the **differential mode**

$$v_d = \frac{v_1 - v_2}{2}$$

is proportional to the offset between the sensor head and the guiding tape, being used for guidance purposes,

the **common mode**

$$v_c = \frac{v_1 + v_2}{2}$$

is a measure of the absolute misalignment relative to the metal stripe. It can be used as a criteria to decide if the track has been lost, requiring special recovering actions or manoeuvres.

With the rhombic kinematics platform's configuration, a set of two independent antennas, each one associated with a steering wheel and with an associated differential signal v_d, guarantees the best possible precision estimate at better than $\pm 3mm$ from the center of the metal stripe. This accuracy, together with the distance between the two steering blocks, leads, in normal operation, to a maximum angular deviation from the metal stripe of 0.05°.

The referred steering mechanism, locate the vehicle relative to the metal stripe, irrespectively of the region of the environment. An absolute location, at discrete points, is provided by a bar code or a transponder system installed at floor level at properly defined locations. Besides location estimation, this absolute localization system establishes reference positions where decisions have to be taken (e.g., turn right, turn left, reduce speed) and confirmed by the operator.

3.3 Secondary Navigation

The correct operation of a platform acting with no physical path (LGV or free-roaming vehicle) requires localization relative to a world frame providing a periodic estimate of the vehicle's position x and y and orientation θ. The most recent generation of such vehicles, named as LGV (Laser Guided Vehicles), is already under commercial exploitation, with a number of known installations. As a reference see, for example, [NDC], [AGV-E]. Free-roaming vehicles represent a step further in flexibility when compared with LGVs. While LGVs have to always follow a path previously defined in a CAD system, free-roaming vehicles are able to autonomously leave that path, for example to circumvent an unexpected obstacle placed on top of the project path and to regain the previously planned path.

3.3.1 Regular Operation

The most commonly used localization procedures are based on

- a laser scanner device,

- a set of reflectors installed on the building along the routes,

- the vehicle's on-board processor.

The localization based on a laser scanner inherits a triangulation or related methodology, i.e., the knowledge of the angles with which a minimum number of three targets are detected yields the emitter position and orientation relative to an inertial frame, [Borenstein96], [Everett96].

The laser scanner measures the bearings to the reflectors. These are all identical, made of stripes of retroreflective tape and placed at known, carefully chosen locations. When the laser beam from the scanner hits a reflector it is reflected back into the scanner in the same direction of the incoming light that caused the reflection. This, together with the information of the scanning device angle provided by an internal encoder, yields the particular bearing to that reflector. Theoretically, a minimum number of three properly detected reflectors provide the on-board processor with the necessary information for localization estimation. A schematic representation of the laser scanner device and controller is displayed in Figure 18.

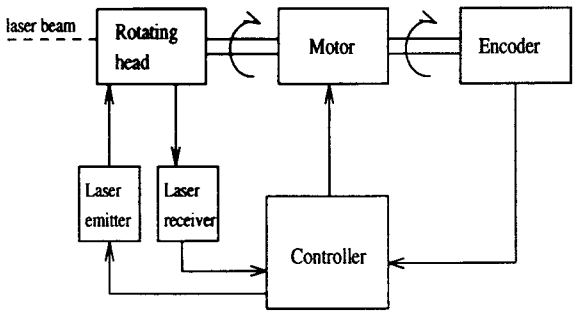

Figure 18: Laser Scanner operation principle

Aiming at reducing the number of reflectors installed all over the building, the laser scanner field of view should not be occluded by the vehicle itself, nor by the cask, pointing towards its installation above the transport cask as schematically represented in Figure 19. The reflectors must be mounted vertically. The height of the reflector must be dimensioned according to the maximum distance to the reflector, the floor conditions and the potential angle deviation of the laser scanner due to the cask load distribution. This height should also account for both situations when the platform is/is not carrying a cask.

The localization estimate supported on a laser scanner and a set of reflectors is a two step approach that distinguishes the estimation of the initial location from the location update during vehicle's motion. This approach, proposed by [NDC] for LGV is also well documented in mobile robotics research work, e.g., [Leonard92], [Arsenio98].

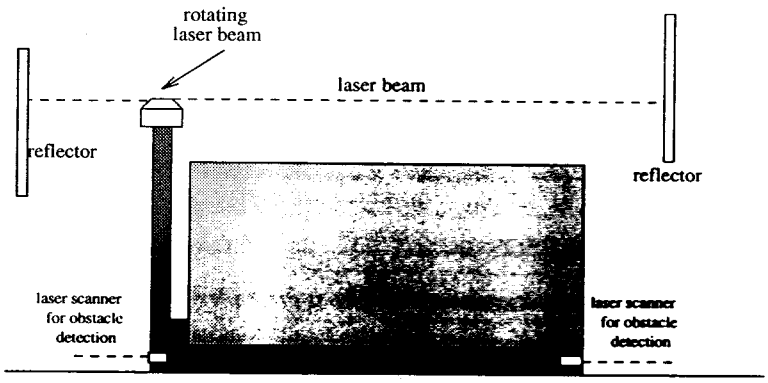

Figure 19: Schematic representation of a Cask and a Transport Platform

The first step estimates the **initial location** and is carried out when there is no a priori information on the platform's location or when the localization error is very large. This step is performed with a still vehicle. In current applications of free-roaming vehicles this initial localization is carried out, for calibration purposes, before starting an operation requiring the vehicle's motion. In the framework of ITER this might not be the case, given that, at the docking ports either at the TB or the HCB, accurate localization is provided by the docking procedures. The bearings from an entire revolution of the laser scanner are used, together with the knowledge of the map location of the entire set of reflectors of the environment, in a matching procedure that yields position and orientation estimates with high accuracy. Data redundancy associated with this initial procedure guarantees estimation robustness against false reflections from targets other than the installed reflectors or reflectors missing due to occlusions induced by unexpected obstacles.

The second step is a **continuous location estimate** applied during motion, and is based on filtering procedures, as schematically represented in Figure 20. In this mode a single bearing, or a few number, is used to update the estimate. The information from the encoders associated with each drive/steering wheel is used, in a dead-reckoning procedure, to roughly predict the platform's location. This location prediction and the location of the reflectors provided on the map yields a prediction of the bearing(s) with which one (or more) reflectors will be detected. A matching procedure that statistically compares the predicted and the observed bearings discards measurements originated from false reflectors or, in an extreme situation, reveals a large error on the location prediction given by the odometric system. If the number of valid matches is small, the platform should stop and the localization algorithm initial step should be in charge of localization. Otherwise, a Kalman filter procedure evaluates a new updated location estimate without requiring any change on the speed of the platform.

In the localization system software, the matching procedure should implement a **safety** system that stops the vehicle if the number of reflector bearings is too low or if the **number**

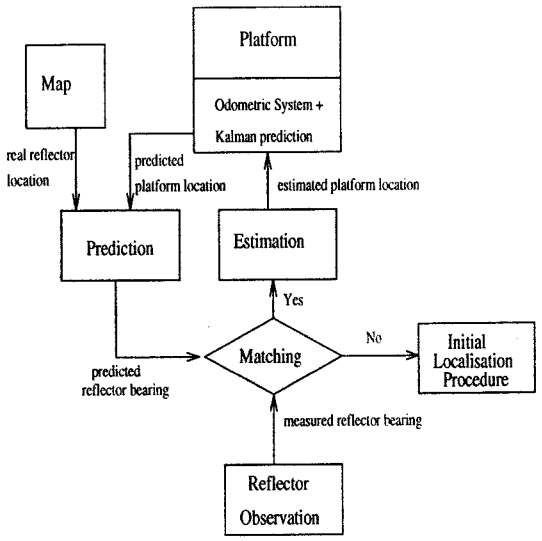

Figure 20: Second step of the Localization algorithm

of bearings to false reflectors are too high. Those are situations that will lead to a small or null number of matchings pairs as displayed in Figure 20 requiring the activation of the Initial Localization procedure.

The resolution of the encoders that support the dead-reckoning system, and the number and placement of the reflectors are key issues on this localization procedure. Encoder resolution will directly condition the deterministic error of the odometric system. The localization system developed by [NDC] recommends a resolution of 10 pulses/degree or better (sync-pulse needed) for the steer controller and an encoder without sync-pulse which gives 1-3 pulses/mm for the drive encoder.

Reflectors geometry relative to the platform's location strongly condition the location errors, [Borenstein96], and may, in the limit, prevent the estimate evaluation. For example, if the platform is in the line defined by three reflectors, these will not yield a valid location estimate. Consequently, reflectors placement on the environment must satisfy the following requirements:

- from every possible platform's location, a minimum number of reflectors should be visible, aiming at providing enough sensorial data for an Initial Location Procedure,
- the density of reflectors used for localization purposes during platform's motion, where a single or a few number of bearings are used for location update, should cope with reflectors missing occurrences.

The exact placement of reflectors requires further analysis.

3.3.2 Secondary Navigation used as a Backup

Whenever the platform acts as an AGV type vehicle, navigation will be provided by the metal stripe, and, in principle, no additional on-line navigation procedure will be necessary in the semi-automatic and backup manual modes. In the normal manual mode where no reference by the physical path is used and the operator is driving the vehicle with a joystick, he/she has visual feedback information, either as seen from the platform (cameras on the platform) and/or from the environment (cameras on the environment).

However, to account for any failure of the guidance sensor or on the PLC, or even to better assist the operator in the normal manual mode and to provide him/her quantitative information on localization, we propose to install the so described secondary navigation system that will provide an on-line localization information relative to a world frame. This information will be plotted in a Human-Computer-Interface (HCI) together with the visual display of the metal stripe topology, providing a schematic picture of the platform status relative to the physical path used for monitoring purposes. A detailed description of the HCI is provided in Section 3.4.

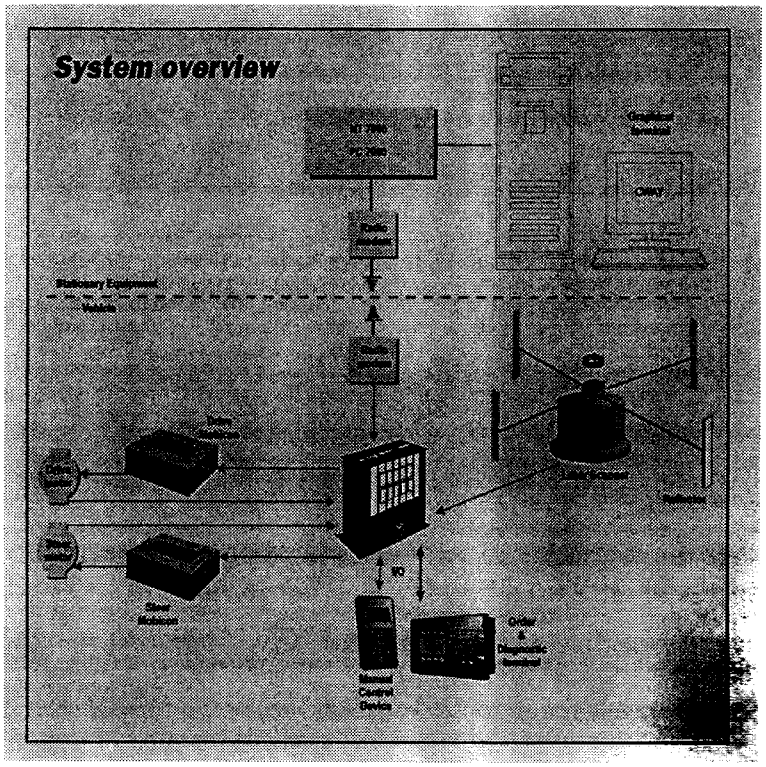

Figure 21: Schematic representation of the Lazerway system from NDC

This scheme will even allow the operation as in the semi-automatic mode in the case of failure of the W-sensor, following the lines of the Lazerway system produced by NDC, (see catalogue in Annex E), and schematically represented in Figure 21 (taken from [NDC]).

In this system, a complete set of virtual paths is generated in a CAD system and downloaded on the platform's on-board controller. To overcome a failure of the W-sensor and even though following the same trajectories as those defined by the metal stripe, these CAD based virtual paths will be coincident with the physical paths. The on-board controller uses the platform's location given by the laser system and the reference path stored in memory (rather than the physical one) to dispatch the correct motion commands to the steering wheels. Drive speed could be defined by the operator as in the proposal of [AeroGo98] or could be automatically defined.

This issue will be detailed in the next subsection where the switching between an AGV type vehicle and a free-roaming vehicle will be discussed.

3.4 Flexible Control Architecture

This subsection proposes an overall control architecture to support different types of operation principles of the transporter platforms. It copes with an AGV-type operation as described in [AeroGo98] including its operational modes (semi-automatic, normal manual, back-up manual), a free-roaming operation principle and a switching mechanism between them. The proposed control scheme is prepared to handle the semi-automatic mode both with a physical or a virtual path. This will provide redundant guidance mechanisms in the AGV-type platform, which might be useful in the case of failure of the W-sensor.

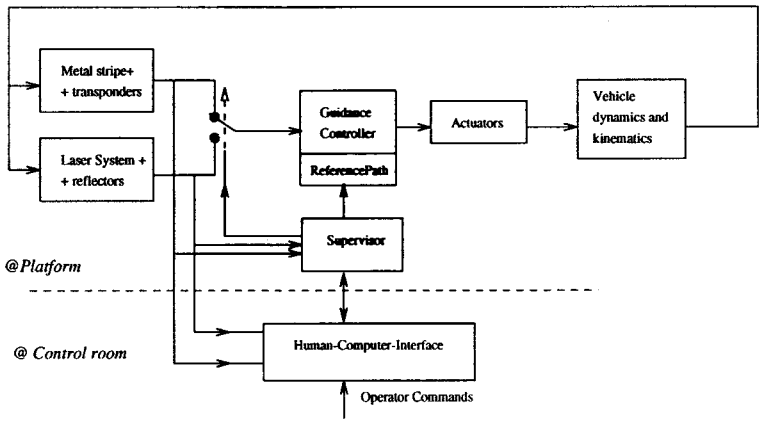

Figure 22: Overall architecture

The architecture, represented in Figure 22, has a set of basic blocks, namely the two navigation systems previously presented. The guidance controller drives the vehicle's actuators aiming at following the reference path. With the properly chosen navigation information and given the reference path, the guidance controller computes the outputs that must be sent as set-points to the actuators in order to minimize the deviation (error) between the vehicle's actual location and the desired one given by the reference path.

The reference path is either the metal stripe defined at floor level or a virtual one defined in a CAD based system prior to operation and downloaded to the platform's controller. Among other roles, and based on a criteria explained later, the supervisor defines which is the reference path to be followed. For reliability purposes, it is envisaged that the topology of the entire physical path routes are generated in a CAD system and downloaded on the platform's controller. For an AGV-like platform operating in the semi-automatic mode, the two navigation and guidance strategies,

$$(W - sensor,\ physical\ path)$$

$$(Laserscanner + reflectors,\ virtualpath)$$

will make the platform follow the path defined by the metal stripe, even though it is not actually used in the second case.

The operation as a free-roaming vehicle in certain situations or particular areas has to be preceded by the evaluation of the desired reference path, followed by its download on the platform's controller. The path design is an iterative procedure, along the following steps:

i) from the platform's actual location displayed on a Human-Computer-Interface, the operator specifies a set of via points or postures and a final goal to be reached by the platform,

ii) an optimization procedure evaluates the optimal path along the via points up to the final goal,

iii) a simulation procedure displays on a screen the area spanned by the platform should it follows the path defined in ii),

iv) if the operator accepts ii) based on iii), the designed path is downloaded on the platform's controller and is taken by the supervisor as the reference path. On the contrary, a new iteration has to be carried out.

On a console displayed at the control room, the operator defines the desired operation mode of the platform. On the normal manual or backup manual modes, no reference path is required. On the semi-automatic mode, the reference path is the physical one and navigation is based on path sensing. On the free-roaming mode the reference path is evaluated beforehand, downloaded on the controller and the navigation is based on the combined use of the laser scanner and the reflectors.

During operation on the semi-automatic mode, the supervisor monitors the value of the common mode, v_c. Should this signal be out of range, meaning that the path is lost (which according to [AeroGo98] is highly unprobable), the supervisor switches the reference path to the virtual path and takes the estimated location from the laser scanner system, keeping the same operation mode. As soon as the physical path is regained, the navigation information will again be given by the W-sensor.

Irrespectively of the operation mode, we propose that the operator be assisted by a Human-Computer Interface (HCI), where major information relative to the platform's status should be displayed and through which the operator commands should be issued.

The following is a minimum set of information that should be included on the HCI for **monitoring** purposes:

- simplified CAD layout of the installation, with the possibility of switching the display between limited areas (e.g., gallery equatorial level, HCB, TB, docking port),
- layout of the metal stripe path topology, superimposed on the environment CAD simplified model (see Figure 23 taken from NDC Laserway navigation system),
- On-line display of the platform (represented for example as a rectangle) based on the estimated localization given by the secondary navigation system (see Figure 24 taken from Laserway navigation system of NDC),
- On-line display of sensorial data associated with the primary navigation,
- On-line display of the range data acquired by the laser scanners installed in the front and rear of the platform for obstacle detection purposes,
- Video images from the cameras on-board the platform and on the environment, with the possibility of choosing the desired camera,
- Monitoring information on the platform's status, e.g., battery level, last detected transponder.

The following is a minimum set of commands the operator should be able to dispatch to the platform's controller/supervisor:

- switching between operation modes,
- controlling the drive wheel speed in the semi-automatic mode,
- driving the platform, with a joystick-like tool, in both the normal manual and the backup manual modes,
- confirm and/or abort specific operations,

3.5 Specification and Cost of Laser Scanner Absolute Localization Systems

This section presents the specification of some commercially available navigation systems to support, up to different extents, some of the navigation features of an LGV or a free-roaming platform, together with an estimated cost. These systems will have to be added and integrated with the equipment proposed by [AeroGo98] for an AGV-type platform. Considerations on the on-board processor need further investigation.

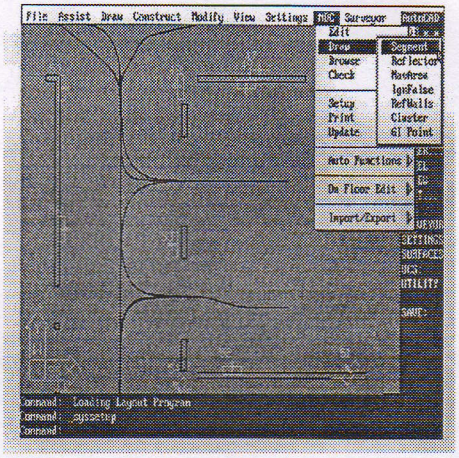

Figure 23: Example of path layout display on the HCI

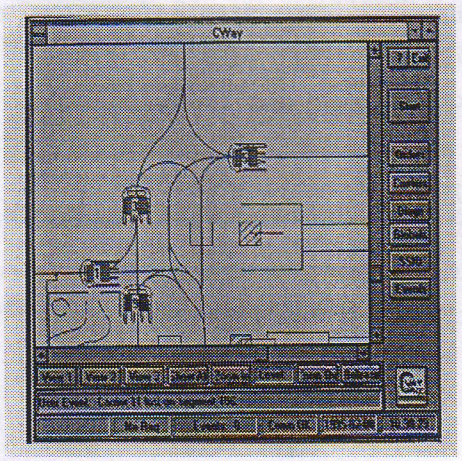

Figure 24: Example of platforms within the environment and displayed on the HCI

3.5.1 Robosense

The following text, included in italic, was taken from Robosense brochure produced by the French company Robosoft.

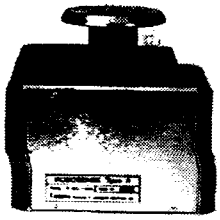

Figure 25: Laser scanner of Robosense

General Features

ROBOSENSE is the state-of-the-art extended-range intelligent navigation system for fast autonomous vehicles. It is built by Siman (a company from Israel) and commercialized in Europe by Robosoft.

Built according to the specifications of leading robot developers, and using Time-of-Flight GaAs Laser technology for range and angle measurements, ROBOSENSE extends the horizons of mobile robots. ROBOSENSE, as an electro-optical navigation system for autonomous vehicles, computer position and orientation by matching the measured instantaneous location with the site map stored in the system's memory.

The system provides navigation data to the vehicle's main computer, where it is processed with the mission planning instruction and the controlling functions to produce the driving and steering commands.

Robosense Technical Specifications

- **Vehicle speed**: *Up to* $3m/sec$, $180°/sec$ *turn rate,*
- **Communication**: *RS-232, full-duplex,*
- **Sizes**: $160 \times 205 \times 170mm$,
- **Weight**: *2.5Kg,*
- **Power**: *24VDC, 1A*
- **Standard features**: *Mapping, Positioning, confidence Level Reporting*

Accuracy

- **Position**: $2.5cm$ *at maximum vehicle speed*

- **Heading**: 0.3°
- **Navigation**: *absolute. No drift*

Processors

- **Laser Controller**: *CPU 8751*
- **Navigation Computer**: *CPU 80386/25MHz*

Laser

- **Type**: *GaAs, pulse*
- **Field of View**: 360°
- **Rotations/Sec**: *10*
- **Range**: *up to 20m*
- **Update rate**: *up to 40Hz*
- **Safety**: *Meets ANSI Z-136, Class 1*

Cost: 69 000 FrF $\simeq$ 11500 USD

Comments:

This system exclusively evaluates the platform absolute location. Contrary to the Laserway system of NDC, Robosense has no associated CAD path planning nor any incorporated guidance controller for a free-roaming platform.

3.5.2 Laserway system

The complete brochure of this system is included in Annex E.

Cost: It was not possible to obtain exact figures directly from the supplier, which recommended a consultation to one of its partners. We plan to do that in the near future.

References

[AeroGo98] E. Vereeken, "Design Study for an Air Floating System", EFET Order ref. N006060/C9579/BK/PJ, AeroGo ref. 30612/98.

[AGV-E] AGV Electronics Web page at URL http://www.agve.se/

[Arsenio98] A. Arsénio, "Active Laser Range Sensing for Natural Landmark Based Localization of Mobile Robots" submitted M.Sc. Thesis, Instituto Superior Técnico, Technical University of Lisbon, Portugal, January 1998.

[Borenstein96] J.Borenstein, H.R.Everett, L.Feng, "Navigating Mobile Robots" A.K. Peters, Ltd, Wellesley, MA, 1996.

[Everett96] H. R. Everett, "Sensors for Mobile Robots" A.K.Peters, Ltd, Wellesley, 1996.

[Hammond86] G.Hammond, "AGVS at Work: Automated Guided Vehicle Systems," IFS Publications, 1986.

[Kanayama90] Y. Kanayama, B. Hartman, "Smooth Local Path Planning for Autonomous Vehicles", in *Autonomous Robot Vehicles*, editors I. Cox, G. Wilfong, 1990

[Kanayama] Y. Kanayama, N. Miyake, "Trajectory Generation for Mobile Vehicles"

[Leonard92] J. Leonard, H. Durrant-Whyte, "Directed Sonar Sensing for Mobile Robot Navigation," Kluwer Academic Publishers, 1992.

[NNC98] "Air Flotation Transport System from the Tokamak Building to the Hot Cell Building - Design Feasibility Report", Report of ITER Task Number EU-D311, NNC, March 1998.

[IST97] M. Isabel Ribeiro, Pedro U. Lima, Pedro M. Aparício, Renato M. Ferreira, "Conceptual Study on Flexible Guidance and Docking Systems for ITER Remote Handling Transport Casks," final report of the contract No.ERB 5004 CT 96 0127 - NET/96-431 between the European Atomic Energy Community and the EURATOM/Instituto Superior Técnico Association, July 1997.

[IGDR] "ITER General Design Requirements," March 96.

[DDC] "Technical basis for the ITER Detail Design Report (DDR)," Draft, November 1996.

[DDD 6.2] K. Ishimoto, E. Tanaka, "Design Description Document - 6.2 - Buildings," November 1996.

[DDD] "Design Description Document - Remote Handling Equipment," November 1996.

[NDC] Netzler & Dahlgren Co News, No.8, No.9 and No.10 and Web page with URL http://www.ndc.se/

[NNC98] NNC, "Air Flotation Transport System from the Tokamak Building to the Hot Cell Building - Design Feasibility Report,Report of ITER Task Number EU-D311, March 1998.

[Nuyts] Nuyts, "W-Sensor. Specification sheet".

[JAHT] E. Tada, "Status of Component Transfer Design and R&D" Viewgraphs distributed at the Remote Handling Co-ordination Meeting, Garching, January 13-14, 1997.

A Rhombic Platform Kinematic Configuration

Mobile vehicles with a rhombic kinematic configuration are commonly used in industrial environments as Automated Guided Vehicles (AGV) or free roaming robots. This kinematic structure has several advantages over other kinematic structures, namely:

- improved manoeuvrability
- ability to assume several different kinematic configurations and
- simple control of the turning radius.

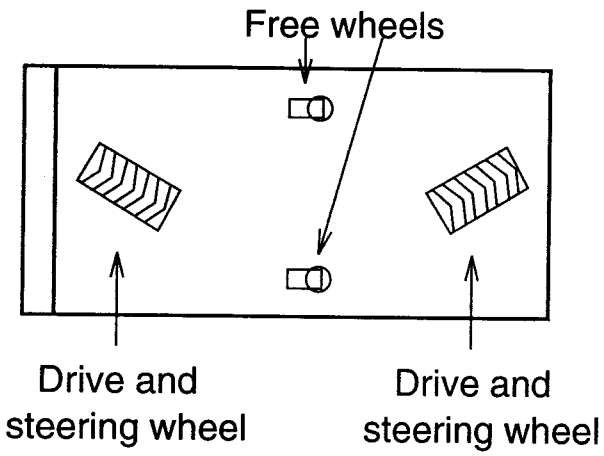

Figure 26: Schematic representation of a rhombic vehicle.

A typical rhombic structure is represented in Figure 26. It consists of two independent drive units placed in the front and in the rear of the vehicle (respectively denoted by the subscripts f and r in the sequel).

The double drive units have the capability to drive and steer the associated wheel. One or both drive units may be used simultaneously. When using both, special care must be taken to assure that the wheels are rotating at compatible speeds, so that neither structural damage of the vehicle nor slippage of the wheels occur. There are commercially available solutions to overcome this problem.

The simultaneous actuation of both steering mechanisms is the correct option in most operation scenarios, to force both wheels to closely follow a pre-specified path (either physical for an AGV or virtual for a free roaming vehicle). Particular path topologies may, however, require an inappropriate combination of steering angles for the two wheels. and should therefore be avoided.

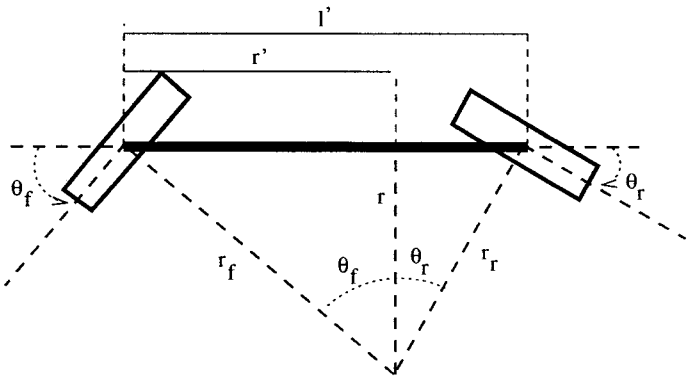

Figure 27: Kinematic Structure of a Rhombic Vehicle

One important issue involved in the design of a rhombic vehicle is the distance l' between the steering axes (double drive units). This has a major influence on the vehicle's turning radius.

From Figure 27, the following geometric equalities are obtained:

$$r_f \cos(\theta_f) = r_r \cos(\theta_r) = r \tag{1}$$

$$l' = r_f \sin(\theta_f) + r_r \sin(\theta_r) \tag{2}$$

where l' denotes the distance between the double drive units, θ_f and θ_r denote the front and rear steering angle, respectively. In this configuration, the vehicle rotates around a point that, at each moment, is defined by the intersection of the lines r_f and r_r in the figure.

As stated before, in the general case both wheels are steerable. This means that the vehicle may assume several different kinematic configurations. For example, if one of the steering angles is kept zero while moving, the vehicle behaves as a tricycle (e.g., $\theta_r = 0$, where θ_r denotes the steering angle imposed to the rear wheel).

One of the advantages of a vehicle with this kinematic configuration is its ability to assume several kinematic configurations, namely:

C1 - Rhombic vehicle with $\theta_r = \theta_f$ - This is the ideal configuration for the vehicle to follow straight lines or circular arcs centered on the intersection of the lines r_f and r_r. a particular case of which is to turn on the spot (when $\theta_r = \theta_f = 90°$).

C2 - Tricycle configuration - Configuration where either θ_f or θ_r are set to zero. In this situation the vehicle assumes a tricycle configuration (see Figure 29).

C3 - Rhombic Vehicle with $\theta_f \neq \theta_r$ - This is the most flexible configuration, since the steering wheels are free (subject only to mechanical constraints) to rotate.

C4 - Rhombic Vehicle with $\theta_f = -\theta_r$ - Configuration that keeps the wheels parallel to each other, allowing sideways ($\theta_f = \pm 90°$) or, more generally, "crab motion.

In the following subsections, the three configurations and their particular features are studied with more detail.

A.1 Configuration C1: Rhombic Vehicle with $\theta_f = \theta_r = \theta$

When $\theta_r = \theta_f$, the vehicle can only move along circular (e.g., such as during gallery travel) or straight lines. This implies that trajectories which, by its nature, are not a sequence of straight lines and circular arcs, have to be decomposed in sub-trajectories composed of straight lines and circular arcs. As such, whenever trajectory type changes (e.g., moving from a straight line to a circular arc) there will be discontinuities in the steering angles required to the vehicle, due to discontinuities in the first derivative of the vehicles longitudinal axis heading angle. This may lead to oscillations around the desired trajectories.

From (1), equal steering angles yield $r_r = r_f = r$. Using (2), with $\theta_f = \theta_r = \theta$, ($\theta \neq 90°$) one can easily obtain a relation between l', θ and r, given by:

$$l' = 2r \sin(\theta) \tag{3}$$

With that configuration, the curvature radius r of the vehicle trajectory is related to the steering angle through equation (3)):

$$r = \frac{l'}{2\sin(\theta)} \tag{4}$$

From the curvature radius of a circular arc path to be followed by the vehicle, the corresponding steering angles are given by:

$$\theta = \arcsin(\frac{l'}{2r}) \tag{5}$$

Equation (4) states that the curvature radii this particular rhombic vehicle is capable of, depends on the distance l' between the steering wheels and on the maximum angle that the steering mechanism can produce, θ_{max}. Thus, the minimum radius of curvature that the vehicle can cope with is given by:

$$r_{min} = \frac{l'}{2\sin(\theta_{max})} \tag{6}$$

Figure 28 presents some radii of curvature obtained for different steering angles ($\theta = \theta_f = \theta_r$) and distance between axes. In this figure only the angles between 15° and 75° are presented. Those are the ones which allow smaller curvature radii, an important feature to change from a circular path to a radial one, as it is the case when the vehicle prepares to dock to the VV. Note that the values presented in the figure refer to the distance between the wheel contact point and the center of rotation. Commercial (e.g., Schabmüller) double drive units allow a maximum turning angle of ±105° per steering wheel.

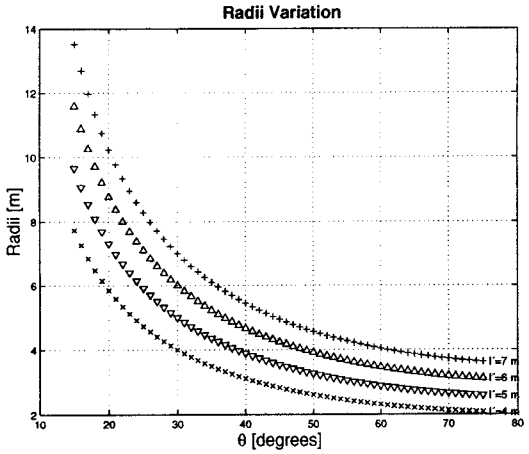

Figure 28: Curvature Radius of a rhombic platform with $\theta_r = \theta_f = \theta$ *vs* θ and l'

From Figure 28 it is clear that:

- For the same steering angle, the curvature radius decreases (narrower curves) when the distance between wheel axes, l', decreases;
- For a constant l', the described curvature radius decreases when the steering angle increases.

A.2 Configuration C2: Tricycle Vehicle - free θ_f, $\theta_r = 0$ (fixed)

In this particular rhombic structure, one of the steering angles is fixed to zero (usually, the rear wheel). Vehicle steering is accomplished through the other wheel, which usually also acts as the traction wheel. This results in a well known industrial kinematic configuration, known as the tricycle configuration.

Making $\theta_r = 0$ and referring to Figure 29, the following geometric equalities arise:

$$l' = r_r \tan(\theta_f). \tag{7}$$

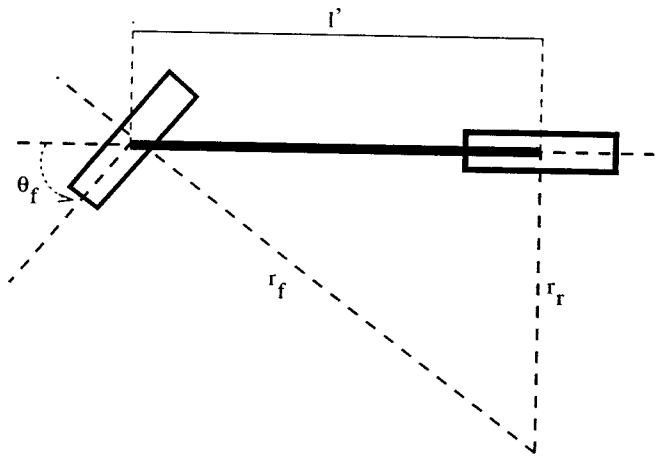

Figure 29: Kinematic structure of a rhombic vehicle with tricycle configuration

As such, the curvature radius of the vehicle trajectory has two components: the front wheel radius and the rear wheel radius, respectively given by

$$r_f = \frac{l'}{\sin(\theta_f)}. \tag{8}$$

$$r_r = r_f \cos(\theta_f) = \frac{l'}{\tan(\theta_f)}. \tag{9}$$

Equation (9) shows that the trajectory curvature radius will increase to infinity (motion along a straight line), as the steering angle decreases to zero.

Figure 30 presents simulation results where, for different distances l' between the driving units, the two curvature radii of the vehicle trajectory are plotted *vs* the front wheel steering angle.

Note that, should the rear drive wheel be used as the traction wheel, some of the data displayed in Figure 30 would not correspond to feasible configurations, since there is a value of θ_f after which the rear wheel will slip.

A.3 Configuration C3: Generic Rhombic Vehicle - free θ_f, θ_r

The generic rhombic configuration uses the independent steering wheels placed in the vehicle front and rear (see Figure 27).

When using front and rear steering sensors, this configuration shows a small tracking error while following a track. These vehicles have the capability to change direction in limited spaces and thus may change between radial and circular paths with both wheels aligned with the path. In the most general case, each steering wheel is associated with a

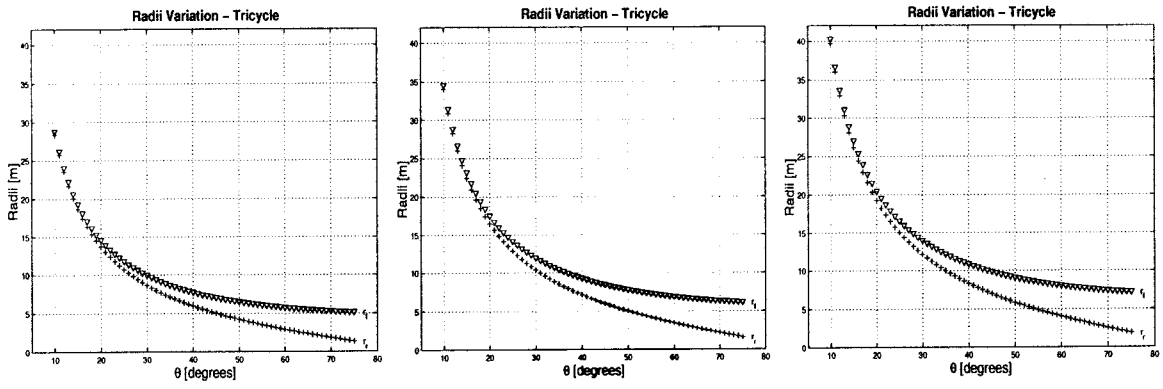

a) $l' = 5m$ b) $l' = 6m$ c) $l' = 7m$

Figure 30: Curvature radii r_r and r_f *vs* $\theta = \theta_f$ for the tricycle configuration, for different distances l' between wheels

different steering sensor and the angles θ_r and θ_f are usually different, as they depend on the path topology.

A closed form expression for the curvature radius of the trajectories followed by such a vehicle can be obtained. Given l', θ_f and θ_r in Figure 27, and equations (1) and (2), the following geometric equalities yield,

$$\begin{cases} r_r = \frac{l'}{\cos(\theta_r)\tan(\theta_f)+\sin(\theta_r)} \\ r_f = r_r \frac{\cos(\theta_r)}{\cos(\theta_f)} \\ r = r_f \cos(\theta_f) \\ r' = r_f \sin(\theta_f) \end{cases} \tag{10}$$

The system of equations (10) allow the computation of the vehicle trajectory radius r (see Figure 27) as a function of l', θ_f and θ_r.

As stated before, note that not all configurations are possible to implement. This comes from the fact that, when both drive units are not used at the same time, there are some steering configurations that lead to wheel slippage.

B Rescue Space for a Rhombic Platform

Considering a vehicle composed by a platform transporting a cask, platform removal under a rescue scenario is only possible if there is enough clearance. In this study, it is assumed that the platform is not flexible and can only move in a straight line along its longitudinal axis when coming out or entering below a cask. In other words, no other type of manoeuvres of the platform when moving underneath the cask are considered. Assuming a stopped cask aligned or not with a physical path, the goal of this section is to derive the mathematical framework aiming at evaluating the maximum space available along a straight line, so that an entire platform or (in the case of multi-body platforms) a part of it, can be removed. We will consider two critical zones in this study: the TB gallery and the HC Transport Corridor.

B.1 In the Gallery

When moving along a circular path in the TB gallery, the best kinematic configuration is the one that establishes $\theta_f = \theta_r = 4.88°$ (case C1 in Appendix A), i.e., supporting motion along a circular arc path with radius = 37m. Therefore, the vehicle may be assumed to move such that its longitudinal axis is always perpendicular to the building radius (see Figure 31).

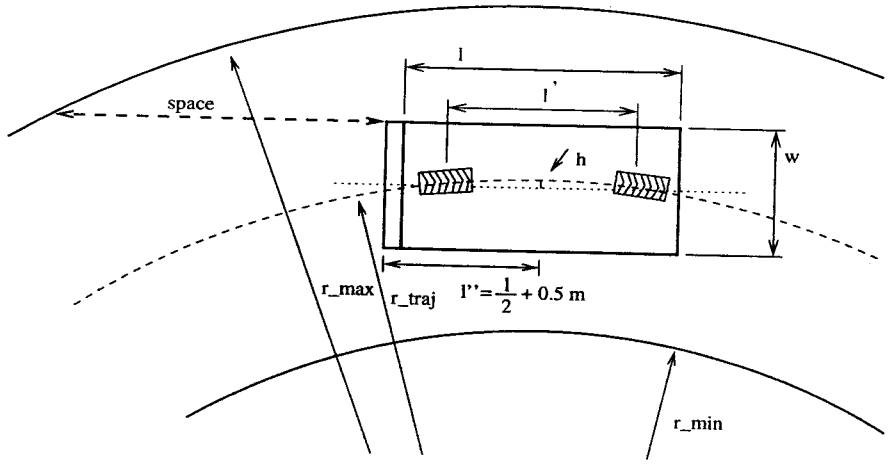

Figure 31: Rhombic vehicle in the gallery, perfectly aligned with the circular path.

With the vehicle perfectly aligned with the path, its center (the intersection of the two diagonals) will travel at a distance h from the path, as shown in Figure 31. The path radius can be obtained from the values for the maximum and minimum radius in the gallery. Considering $r_{max} = 42m$ and $r_{min} = 32m$, r_{traj} is $37m$. This value guarantees that the vehicle travels in the middle of the available space (on a radial criteria).

The displacement of the vehicle center with respect to r_{traj}, h, is given by:

$$h = r_{traj}[1 - \cos(\theta)] \tag{11}$$

where θ is the absolute value for the steering angles and r_{traj} represents the curvature radius of the desired path.

In the sequel, we evaluate the free space available in the vicinity of the vehicle, when stopped in the gallery, under two scenarios: aligned and unaligned with the track.

Vehicle aligned with the track

When travelling along a circular path, either physical or virtual, and assuming perfect alignment relative to the reference path, the entire platform cask will not collide with the interior wall of the gallery should the following condition hold:

$$r_{traj} - h - \frac{w}{2} > r_{min} \tag{12}$$

The clearance over a straight line ahead of the vehicle is measured by the variable *space*, which satisfies the condition:

$$\sqrt{(r_{traj} - h + \frac{w}{2})^2 + (l'' + space)^2} < r_{max} \tag{13}$$

or, stated in order to *space*:

$$space = \sqrt{r_{max}^2 - (r_{traj} - h + \frac{w}{2})^2} - l'' \tag{14}$$

Vehicle unaligned with the track

Although air-cushion mobile systems are reliable and stop immediately in case of air compressor failure, one must consider the occurrence of a very unlikely scenario under which the vehicle would stop considerably unaligned with the path. Calculations were made to evaluate the available space, under this scenario.

Figure 32 presents a vehicle in the gallery, in a situation where some position and orientation errors are present relative to a perfect circular path. The following calculations lead to the expression that computes the available space as a function of the involved parameters. In this figure, $space = \min(\overline{AA'}, \overline{BB'})$. Figure 33 presents a schematic representation of the alignment error presented in Figure 32.

From Figure 32,

$$x = \frac{w}{2}\tan(\beta) \tag{15}$$

$$y = \frac{w}{2\cos(\beta)} \tag{16}$$

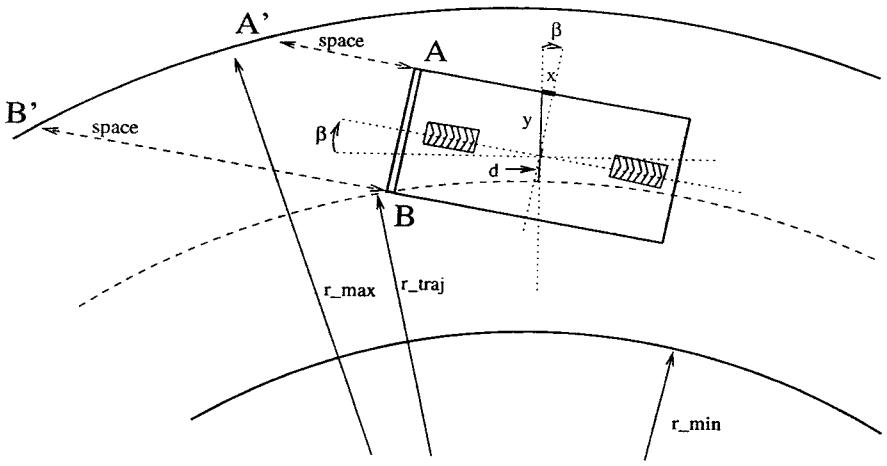

Figure 32: Vehicle alignment errors in the gallery.

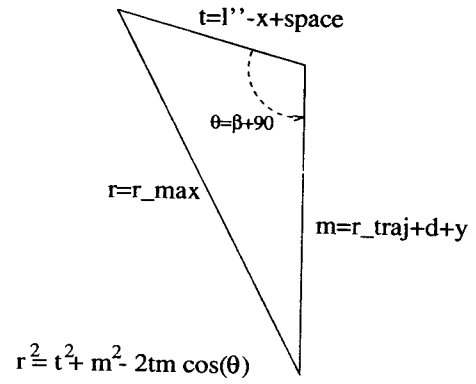

Figure 33: Schematic representation of alignment errors.

where β is the unalignment angle and w is the vehicle width. Using (15), (16) and the cosine law, it is possible to evaluate the available space along the line that is defined by points A and A' in Figure 32. From Figure 33:

$$(r_{traj} + d + y)^2 + (l'' - x + space)^2 + 2(r_{traj} + d + y)(l'' - x + space)\sin(\beta) < r_{max}^2 \quad (17)$$

where d is the deviation from the track of the vehicle center, along the radial direction.

Setting

$$a = r_{traj} + d + y \quad (18)$$

and

$$b = l'' - x, \quad (19)$$

and solving in order to *space* yields:

$$\overline{AA'} = -(2b + 2a\sin(\beta) \pm \sqrt{(b + a\sin(\beta)^2 + r_{max}^2 - a^2 - b^2 - 2ab\sin(\beta))} \quad (20)$$

The space $\overline{BB'}$ is evaluated in a similar way. The difference consists on the redefinition of a and b, which becomes now:

$$a = r_{traj} + d - y \quad (21)$$

and

$$b = l'' + x, \quad (22)$$

Equation (20) defines the available space as a function of the error parameters, with a and b, determined by (21) and (22).

If the displacement relative to the desired trajectory (d) or the orientation error (β) is too large, there may also occur collisions with the interior wall of the galleries. To assess this case, equation (20) is changed, leading to:

$$\overline{BB'} = -(2b + 2a\sin(\beta) \pm \sqrt{(b + a\sin(\beta)^2 + r_{min}^2 - a^2 - b^2 - 2ab\sin(\beta))} \quad (23)$$

where r_{max} in (20) was replaced by r_{min}. If the line that goes out of the vehicle from point B along the vehicle longitudinal direction does not intersect the interior wall of the gallery, the result of the evaluation of equation (23) is $space = \infty$.

B.2 Hot Cell Transport Corridor

Assuming that the guidance and navigation system keep the vehicle wheels within a $\pm 100mm$ range centered on the track, the maximum unalignment occurs when one wheel

is deviated $+100mm$ from the track and the other wheel is deviated $-100mm$. Figure 34 depicts a schematic representation of this situation. In such case, the maximum orientation unalignment is given by:

$$\beta_{max} = \arctan(\frac{max\_deviation}{\frac{l'}{2}}) = 2°. \tag{24}$$

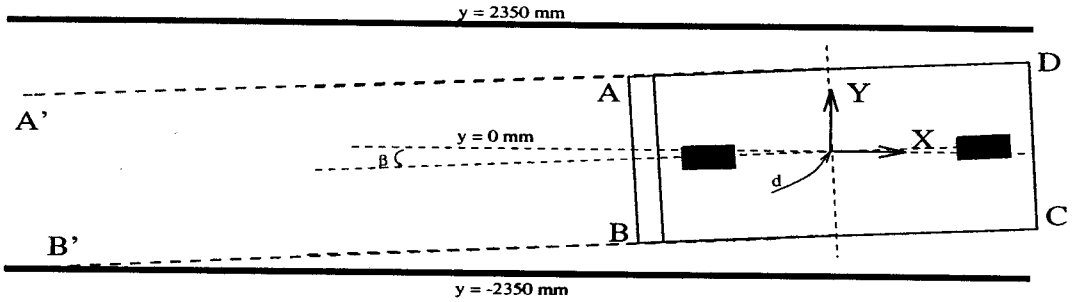

Figure 34: Schematic representation of a rhombic vehicle in the Hot Cell Transfer Corridor. A' and B' represent the intersection of the dashed straight lines (starting in A and B, respectively), with the bottom wall.

If only one wheel is unaligned, the maximum angular error is given by:

$$\beta = \arctan(\frac{max\_deviation}{l'}) = 1°. \tag{25}$$

To calculate the available space to perform rescue manoeuvres, it is necessary to know the position of the vehicle corners. With this purpose, a reference frame was fixed to the vehicle, as depicted in Figure 34. If the vehicle frame is rotated $\beta°$ with respect to a frame whose origin is above the path, at the height of the vehicle frame, and its origin is deviated d mm from this reference frame (along the perpendicular to the path), the vertex A (A_x,A_y)position is computed from its perfectly aligned position A_a (A_{a_x},A_{a_y}) by:

$$\begin{bmatrix} A_x \\ A_y \end{bmatrix} = \begin{bmatrix} \cos(\beta) & -\sin(\beta) & 0 \\ \sin(\beta) & \cos(\beta) & d \end{bmatrix} \cdot \begin{bmatrix} A_{a_x} \\ A_{a_y} \\ 1 \end{bmatrix} \tag{26}$$

where the subscripts x and y denote the planar coordinates of a point.

Note that, if there is perfect alignment ($\beta = 0$ and $d = 0$), then A equals A_a.

Similarly, point B is calculated from its aligned position B_a according to:

$$\begin{bmatrix} B_x \\ B_y \end{bmatrix} = \begin{bmatrix} \cos(\beta) & -\sin(\beta) & 0 \\ \sin(\beta) & \cos(\beta) & d \end{bmatrix} \cdot \begin{bmatrix} B_{a_x} \\ B_{a_y} \\ 1 \end{bmatrix} \tag{27}$$

The straight line that links points A and D has the same slope m of the line that links points B and C, given by:

$$m = \tan(\beta) \tag{28}$$

Given point (A_x, A_y), determined from Equation (26), and the slope m, determined from (28), the intersection of the line that links points A and D with the y-axis is computed as:

$$b = A_y - m \cdot A_x. \tag{29}$$

The intersection of this line with the walls is now easy to compute. For instance, for point A', A'_y is either 2350 mm or -2350 mm (recalling that the reference frame origin is on the track, equidistant from the walls). One of these values is used, according to the sign of β. From this, we can determine

$$A'_x = \frac{A'_y - b}{m} \tag{30}$$

As such, the space available for manoeuvres, from corner A to A', is given by:

$$\overline{AA'} = \sqrt{(A_x - A'_x)^2 + (A_y - A'_y)^2} \tag{31}$$

Similarly, from corner B to B',

$$\overline{BB'} = \sqrt{(B_x - B'_x)^2 + (B_y - B'_y)^2} \tag{32}$$

Hence, the available clearance rescue *space* is given by:

$$space = \min(\overline{AA'}, \overline{BB'}). \tag{33}$$

C Area Spanned by a Rhombic Platform in the TB Gallery

When moving along a circular path in the gallery, the best kinematic configuration for operation is the one that makes use of equal θ_f and θ_r (case C1 in Appendix A). Figure 35 presents a schematic representation of a vehicle traveling in the gallery.

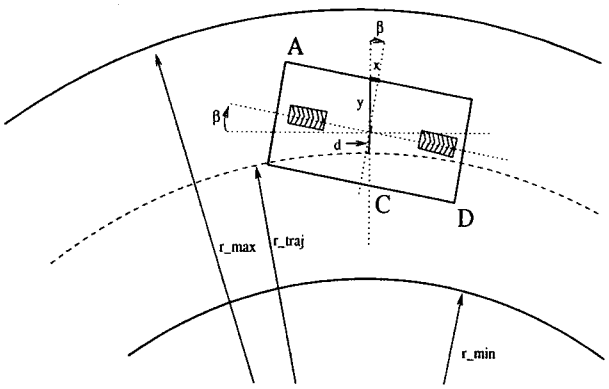

Figure 35: Rhombic vehicle travelling in the gallery — spanned area.

When the vehicle follows the middle circular path in the galleries, each point of the vehicle border will describe a circular arc, on concentrical circumferences, around the center point of the path (O), located at the center of the TB. Assuming a situation with very small guidance errors, i.e., both steering wheels will be very close to the physical circular path, the vehicle points will describe circular arcs.

Figure 35 shows a rhombic vehicle travelling in the gallery. It spans an area that, besides the path followed and vehicle dimensions, depends on the localization errors. The point that will travel closest to the exterior wall of the gallery is point A in Figure 35. The distance between this point and the center O of the circular path is given by:

$$\overline{OA} = \sqrt{(r_{traj} + d + y)^2 + (\frac{l}{2} - x)^2 + 2(r_{traj} + d + y)(\frac{l}{2} - x)\sin(\beta)} \qquad (34)$$

Notice that x and y are given by the expressions (15) and (16) in Appendix B. Referring to Figure 35, the point of the vehicle that travels closest to the interior wall of the gallery is either point C or D, depending on the value of β. Its distance to the center of the path is given by:

$$\overline{OC} = r_{traj} + d - y \qquad (35)$$

Point D in Figure 35 is relevant to the evaluation of the spanned area by the vehicle.

only in a situation where the angle β is such that $\overline{OD}$ is smaller than $\overline{OC}$. Its distance to the center of the path is given by:

$$\overline{OD} = \sqrt{(r_{traj} + d - y)^2 + (\frac{l}{2} - x)^2 - 2(r_{traj} + d - y)(\frac{l}{2} - x)\sin(\beta)} \tag{36}$$

The vehicle spanned area is the circular band between the circumferences of radii $\overline{OC}$ and $\overline{OA}$ (or $\overline{OD}$ and $\overline{OA}$ for specific values of β). The radii r_{min} and r_{max} are defined respectively by the innermost and outermost limits of the free space in the gallery, according to current building design drawings.

D Cubic Spirals

When moving between two points, if the chosen path is composed of straight lines and circular arcs, the angle of the vehicle steering wheel will be discontinuous at the switching points between those two types of curves. Should a discontinuity exist in the steering angle, the vehicle would not be able to follow the path smoothly. Instead, it would oscillate around the desired path after the line change. To solve that problem, cubic spirals and Cornu spirals (clothoids [Kanayama]) have been widely used in AGV industry, highway and railway curve design, to replace circular arcs. For such curves, the curvature radius changes along the curve, so that its derivative is zero at the switching points.

A cubic spiral [Kanayama90] is a curve whose tangent direction is described by a cubic function of path distance s. The solutions obtained by cubic spirals are smoother than those obtained with clothoids and published results show that the cubic spirals are better in terms of the maximum curvature.

The problem of designing a cubic spiral path can be stated as follows: *Given two poses (position plus orientation), which is the continuous curvature that takes the vehicle from the initial pose and delivers it to the final pose in the smoothest way?* Note that the curvature defines the path along the distance to be covered.

Although no dynamic considerations were made, the cost function used to plan the path can be interpreted from a dynamics viewpoint. Assuming constant velocity of the vehicle along the path (π), the cost function can be seen as the integration of the jerk (variation of angular acceleration) along the path. Since jerk should be minimized to smooth the vehicle motion, the resulting control law will be appropriate for ITER vehicles, due to the safety requirement.

$$Cost(\pi) = \int_0^{\ell} \ddot{\theta}^2 ds \tag{37}$$

where ℓ is the path length.

Note that, some of the path planning problems have to be divided in two trajectories, in order to minimize the total path cost. An analytical form exists to perform the splitting operation in a optimum way, i.e., ensuring that the splitting point is the one that minimizes the total cost. This was done in some examples in this report.

E Lazerway System

Laser navigation for automated vehicles

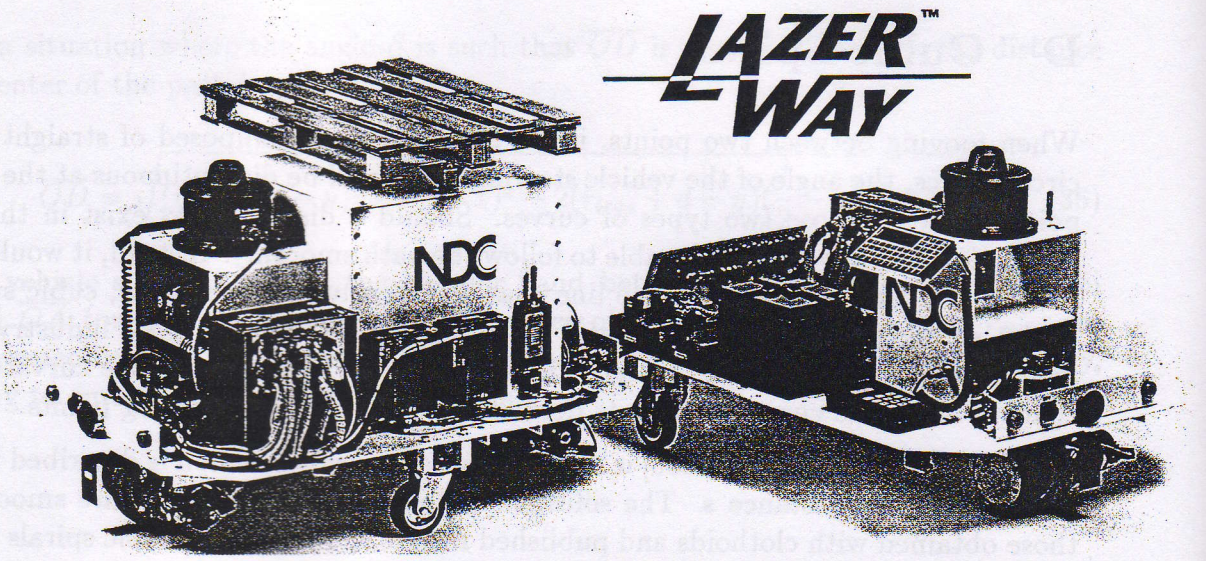

Two of NDC's demonstration / education vehicles; to the left a dual steer / drive vehicle (QUAD) with load handling. To the right a single steer / drive vehicle.

Lazerway navigation is a combination of laser measurement and odometry. The onboard laser scanner detects the position of simple, standardized reflective strips, mounted on walls and equipment in the proximity of the vehicle driveway.

Lazerway makes it possible to use the standard NDC System Seven for laser navigation.

The **Lazerway** enables free range navigation i.e. physical floor reference points, wires or position-IDs are not required.

Through a wide range of extra features, extensive support and high reliability, the NDC vehicle controller (ACC70) provides great possibilities for LGV systems. The ACC70 offers modular solutions for advanced vehicle control and load handling.

Using the ACC70, the vehicle can be controlled in four different steer modes:

- Single steer/drive
- Dual steer/drive
- Differential drive
- Quad directional drive

The ACC70 supports radio and IR communications for laser guided systems.

It also supports continuous full-duplex inductive communication which is standard for wire-guided systems.

Optional serial communication ports are available that support different protocols e.g. for bar code scanners.

The ACC70 also has powerful PLC-support including timer functions able to handle up to 86 digital I/Os.

Additional I/Os are installed by using I/O expansion units.

A map of the entire route layout is stored in the ACC70, which means that the vehicle can find a path to any destination in the layout by itself. The navigation map is easily generated from a CAD drawing with the Layout & Reflector Definition Program.

The ACC70 offers a wide range of status monitoring and diagnostic procedures for faster and easier troubleshooting. It also supports manual control devices/onboard operator control panels.

The ACC70 is customized for each system's specific requirements with the ACC70 Definition Program.

All definition programs run on standard PC models.

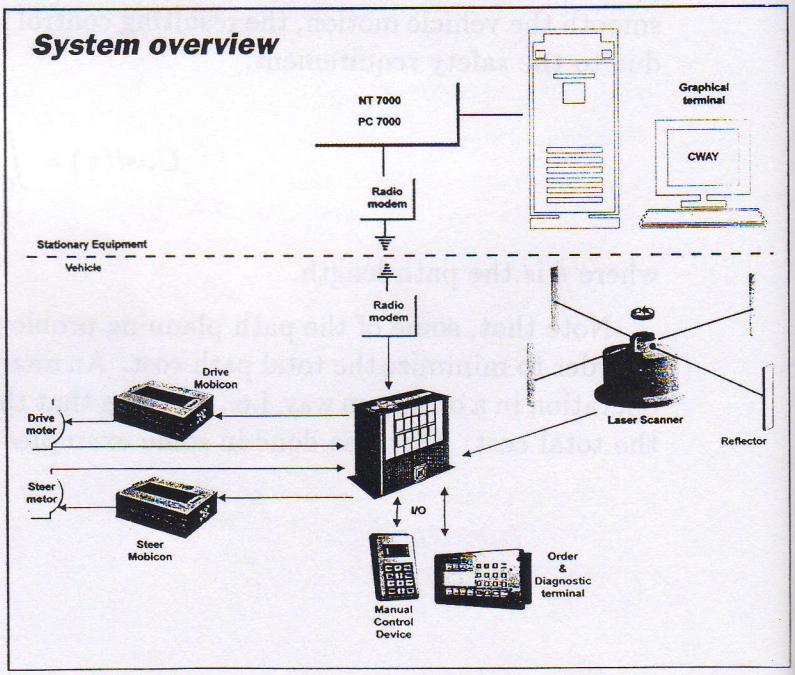

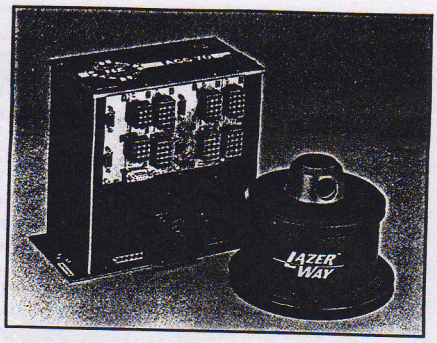

Laser System Features

- Modular configuration
- Wide range of PLC support
- All parameters software defined and user changeable
- Can be used on all floor types
- Suitable for "Clean Room" installations
- Increased route handling capability
- No floor cutting
- Easy to modify the route layout
- Simple reflective tape strips for guidance
- Operates on both 24 and 48 V DC

ACC70 Cards
MPMC II
Multiport memory controller with Central Memory module for all definitions and internal communication.

1 serial interface for definition download (RS-232).

SYS Control Card
System controller card for supervision, master communication, routing (route selection via the layout) and PLC functions.
2 serial interfaces (RS-422 / RS-232)

NAV Card
Laser navigation functions.

2 serial interfaces for the laser scanner (RS-422 / RS-232)

REGCOM Card
Vehicle control functions, including outputs for servo amplifiers and encoder inputs, serial interface for radio/IR communication and Multidrop communication for auxiliary NDC equipment.

- 4 analogue outputs (-10 V - +10 V)
- 4 incremental inputs (two with zero pulse)
- 4 analogue inputs 0-30 V / -15 V - +15 V
- 1 serial interface (RS-232)
- 1 serial interface (RS-485)

I/O 15/14 Card
Digital I/O card including PLC and timer functions.

15/14 digital inputs/outputs

***I 30* Card**
Digital input card including PLC and timer functions.

30 digital inputs

CIO Card
Communication I/O card, including serial interface for radio/IR communication, extra serial interfaces for optional communication, digital I/Os, encoder inputs and multidrop communication for auxiliary NDC equipment.

- 2 serial interfaces (RS-232)
- 1 serial interface (RS-485)
- 2 incremental encoders (with zero pulse)
- 8/6 digital inputs / outputs (optional analogue inputs, 0 - 30 V)

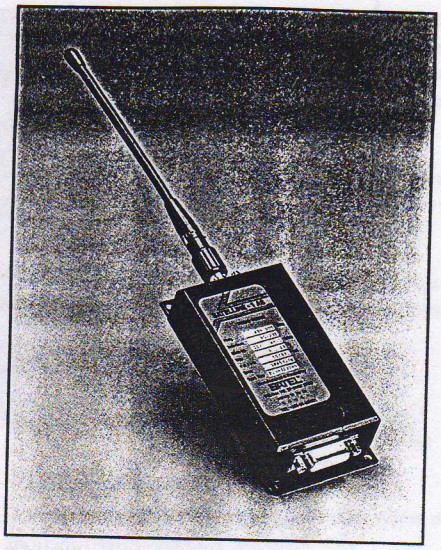

Radio Data Modem Satelline - 1AS

The Satelline-1-AS incorporates a transmitter, receiver and the appropriate modem in one unit, all in one state-of-the-art casing. It is connected via an RS-232 interface to the ACC70 Vehicle Controller and to the stationary Master Controller.

Low weight and small size make the Satelline-1AS easy-to-place anywhere.

The Satelline-1AS operates in the 450 MHz band. It has one crystal-controlled channel which is factory selected. The data transfer rate is 4 800 bits/s as asynchronous data.

Technical Data

Power requirements

Laser Scanner : 24 V DC ± 10 % , 1A

ACC70 : 24/48 V DC ± 30%

ACC70 max power consumption: 25W

Communication data

Radio communication: from 4800 to 9600 Baud

IR communication: 19200 Baud

Operational data

Temperature: 0 to 46° C (32 to 113° F)

Relative humidity: non-condensing 10 to 90%

Laser Scanner

Laser type:	GaAs
Wavelength:	780 nm
Beam diameter:	3mm
Beam divergence:	0.3 mrad
Rotation/sec:	6 r.p.s

Laser classification (EN 60825-1 : 1994)

Class 1:	Output power: 0.1 - 0.6 mW
	Range: up to 45 m
Class 3B:	Output power: 0.1 - 2.5 mW
	Range: up to 65 m

Laser Scanner ver. 1.6 Dimensions:

Diameter: 188 mm

Height: 154 mm

Weight: 2.7 kg

ACC70 II Dimensions (mm)

Top view

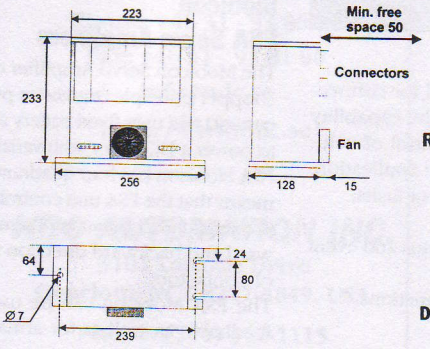

Technical Data Radio Modem Receiver

Receiver

Frequency range: 420-470 MHz

Channel separation : 25 kHz

Number of channels: 1

Transmitter

Frequency range: 420-470 MHz

Carrier power: 400 mW/ +26 dBm/50 ohm

Number of channels: 1

Transmitter

Frequency range: 420-470 MHz

Carrier power: 400 mW

Radio Modem

Temperature range: -25° C to +55° C

Data speed: 4800 bits/sec

Operating voltage: +10 - +13 V DC

Dimensions and weight

Height: 110 mm

Width: 65 mm

Depth: 26 mm

Weight: 280 g

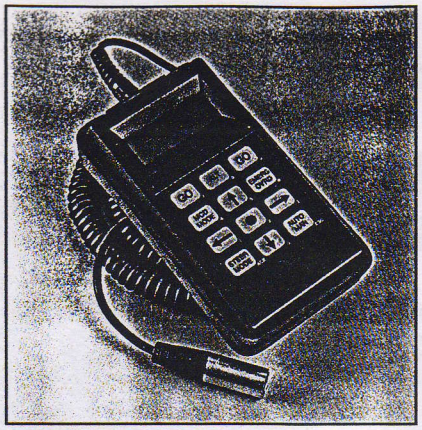

MCD
Manual Control Terminal

The MCD makes it possible to manually control both the steer and drive functions on the load handling equipment of a laser guided vehicle. The MCD is connected to the ACC70 vehicle controller via one plug-in chassis connector.

The MCD has four different modes:

Automatic mode. The LGV is independent of any instructions from the operator/MCD.

Semi-automatic mode. The LGV speed and direction are determined by the user via the MCD. The LGV is automatically guided by the laser to the path. If no path is found, the vehicle can be guided by the operator.

Manual mode. The operator controls all vehicle activities via the MCD. The vehicle is no longer guided by the laser system.

Load handling mode. The operator controls conveyors, lift tables, etc., mounted on the vehicle.

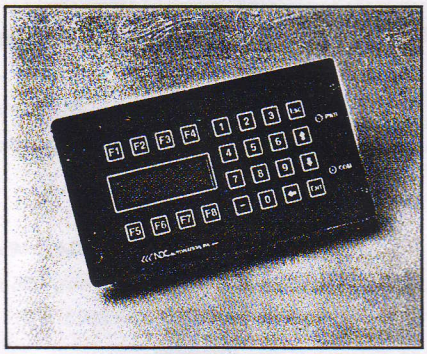

Operator interface

The OP7 is an operator terminal for connection to the ACC70. It increases the capability for manual intervention and control of vehicle functions. Depending on the application, the OP7 can be used for different tasks:

- Supervision of vehicle status and event logging
- Debugging of vehicle functions
- Monitoring I/O status

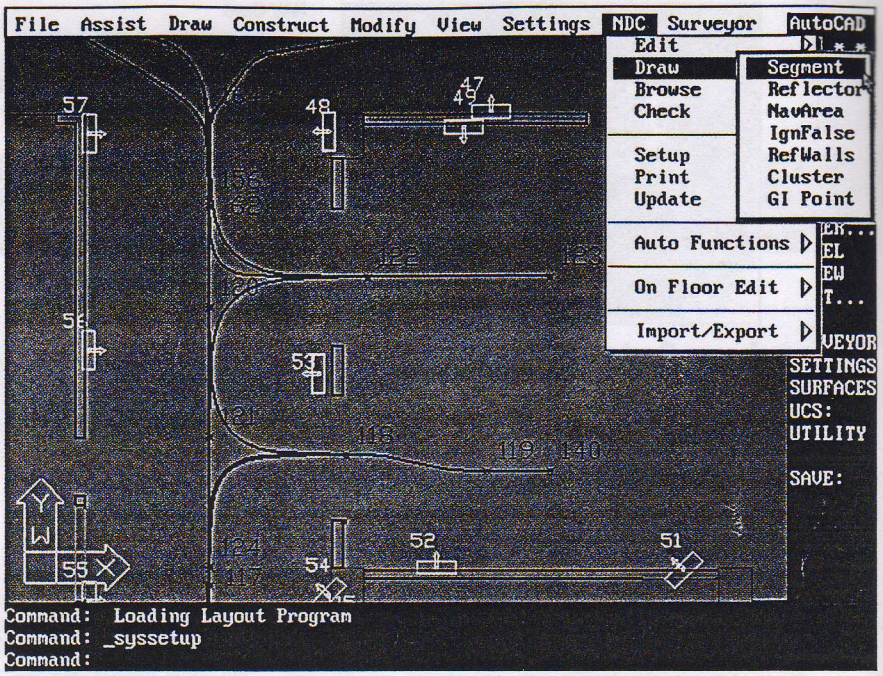

Definition Program

In order to make the application programming of NDC products as user friendly as possible, menu based definition programs are used. There are separate definition programs for the Vehicle controller (ACC70), Master Controller (NT/PC), Operator Interface (CWAY) and Layout (runs under AutoCAD 386 Release 12 for DOS).

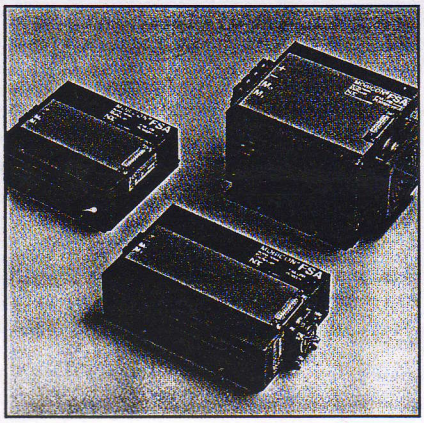

Mobicon
FSA Servo Amplifiers

The Mobicon Servo Amplifier operates on the chopper principle (transistor pulsing of motor current) and uses fixed battery supplied voltage to power a DC motor with variable voltage. The FSA Mobicon has four quadrant control, which means that the FSA unit controls the speed and acceleration/deceleration of a motor in both forward and backward direction without the use of contactors.
The FSA Mobicon can be used for encoder feedback, as well as for armature feedback.

To make the FSA as flexible as possible, all control connections are available externally.

This new Mobicon type FSA is based on Field Effect Transistors (FET), and therefore needs less cooling, which results in a more compact design. The FSA Mobicons are available in the following versions:

FSA23	(23 A max. current / 10 A continuous)
FSA45	(45 A max. current / 20 A continuous)
FSA80	(80 A max. current / 40 A continuous)
FSA150	(150 A max. current / 75 A continuous)
FSA200	(200 A max. current / 100 A continuous)

Features:

- High efficiency, exceeding 90 %
- Variable current limits
- Feedback by tachometer or armature
- Short-circuit protection
- Power transistor over-load protection
- Maintenance free, solid state technology
- Over and under voltage protection
- ESD protection
- Overheating protection
- Forced cooling by fan (FSA45, FSA80, FSA150 and FSA200)

45 A version

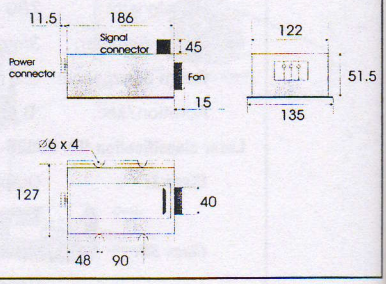

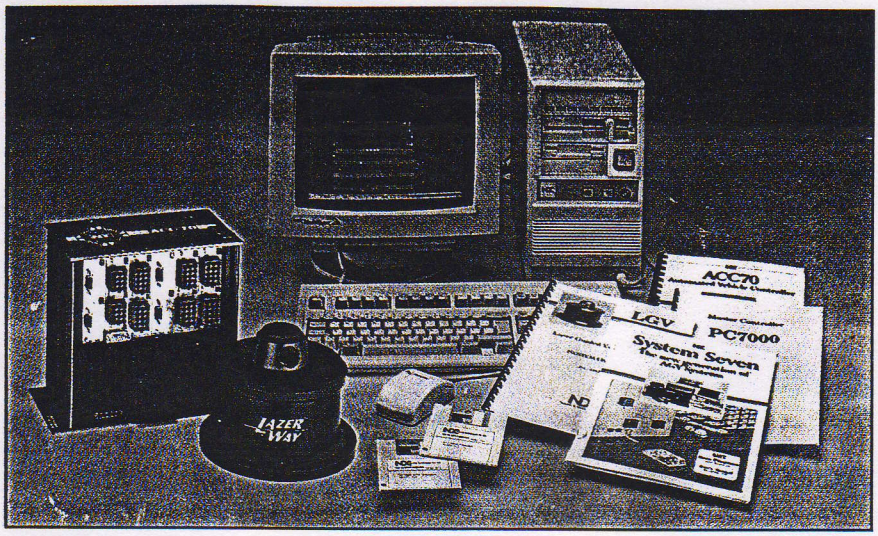

NT 7000

NT 7000 is a Master Controller program for an NDC System Seven for Windows NT 3.5. It is a powerful LGV system order manager and traffic controller. It has advanced diagnostic and statistic functions.

NT 7000 is designed to work with automatic guided vehicles equipped with the ACC70.

The program is run on a standard PC equipped with 1-5 NDC **PC COM card(s)**.

This Master Controller is especially applicable for medium and large sized AGV systems (inductive, laser or other guidance systems) and can be used for stand alone applications, as well as together with a host computer.

NT 7000 controls up to 50 vehicles in the system as standard, and can be expanded.

The 20 communication channels are intended for Host computer communication, vehicle communication (max 16 channels), CWAY and 1–16 multidrop lines for digital I/O units (BIV3, SC7 or SIOX).

Features:

- Has highly sophisticated tools for vehicle control and traffic regulation
- Equipped with various standard protocol drivers for connection of host computers or parallel systems
- Easy to program using the C7 Definition program
- Supports user-defined transport sequences
- Dynamic optimization, allocation and reallocation of traffic
- Built-in system-on-line diagnostics
- Supports CWAY graphic monitoring of the system activities
- Possible to operate in different modes to adapt to around the clock variations in the traffic
- Network communication
- Multitasking environment. CWAY and host software run simultaneously with NT 7000.

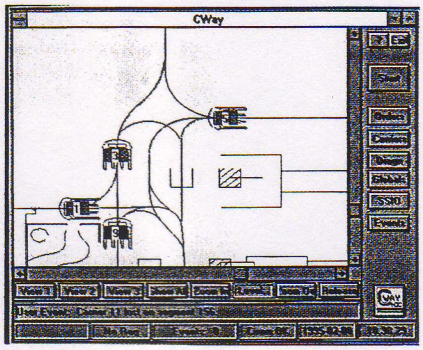

CWAY

CWAY is the operator interface program for an NDC AGV System Seven which runs under MS Windows. The program is used on a standard PC.

Using a layout diagram and tables, CWAY makes it possible for total operating control over the AGV system.

NDC
Netzler & Dahlgren Co AB
SE - 429 80 SÄRÖ SWEDEN
Phone: +46 31 - 93 80 00
Fax: +46 31 - 93 81 00
info@ndc.se
http://www.ndc.se

NDC AUTOMATION INC.
3101 Latrobe Drive
Charlotte NC 28211-4849, USA
Phone: (704) 362-1115
Fax: (704) 365-8468
info@ndca.com
http://www.ndca.com

The graphically displayed layout can be zoomed in 8 preselected levels using command buttons, and also panned in normal Windows fashion. The layout used in CWAY is created by the layout program.

Diagnostic functions at both system and vehicle level ensure good system overview and considerably reduce troubleshooting.

CWAY communicates with the Master Controller via the NetBios networking protocol or serial line.

Features:

- Graphic display of the LGV system generated from AutoCAD drawings
- Total LGV supervision from the graphic display
- Multiple display of different types of tabular data simultaneously
- Excellent diagnostic possibilities on both system and vehicle levels
- Vehicle movement shown in different zoom levels
- Vehicle status clearly displayed with different colours
- Connection with the Master via NetBios or serial line
- Online help

Technical data NT 7000
Communication capacity
Maximum capacity:
20 channels (4 ch/PCCOM card, max. 5 cards)

Software interface
ACI (host computer) interface
CWAY (operator) interface
SSIO interface
Multidrop line
TCP/IP, NetBios

Interface types
Ethernet, TokenRing
RS-432
RS-422
RS-485
20 mA current loop

SSIO lines
Max. 16 channels

Vehicles
Vehicles 50
Vehicle types 8
Numbers of vehicles per type: user selectable

Master parameters
Simultaneous execution, 50 orders
Nodes, 999 per AGV system
Home positions, Selectable
Addressable positions: 2 500, depending on system design

Computer recommendations
Pentium 90, 16 Mb RAM
Diskette drive 3 1/2" 1.44 Mb
One parallel port (1.5 mA at 3V) for NDC Software Protection Device
One full length slot for each PCCOM card (max. 5 cards).

Software Protection
The software is protected by a hardware key (NDC Software Protection Device), which requires a SW Protection key code for the program to start.
The key code is unique for each application and gives access to the purchased system configuration (number of vehicles, etc.)

TH 32081-03